National Bureau of Standards
Library E... ...in. Bldg.
OCT 16 1970

UNITED STATES
DEPARTMENT OF
COMMERCE
PUBLICATION

NBS TECHNICAL NOTE 555

Methods of Measurement for Semiconductor Materials, Process Control, and Devices

Quarterly Report

January 1 to March 31, 1970

U.S.
DEPARTMENT
OF
COMMERCE
National
Bureau
of
Standards

C
0
753
555
70
2.

NATIONAL BUREAU OF STANDARDS

UNITED STATES DEPARTMENT OF COMMERCE
Maurice H. Stans, Secretary
NATIONAL BUREAU OF STANDARDS • Lewis M. Branscomb, Director

TECHNICAL NOTE 555

ISSUED SEPTEMBER 1970
Nat. Bur. Stand. (U.S.), Tech. Note 555, 63 pages (Sept. 1970)
CODEN: NBTNA

Methods of Measurement for Semiconductor Materials, Process Control, and Devices

Quarterly Report
January 1 to March 31, 1970

Edited by W. Murray Bullis and A. J. Baroody, Jr.

Electronic Technology Division
Institute for Applied Technology
National Bureau of Standards
Washington, D.C. 20234

Jointly Supported by the National Bureau of Standards, the Defense Atomic Support Agency, the U.S. Navy Strategic Systems Project Office, the U.S. Navy Electronic Systems Command, and the National Aeronautics and Space Administration

NBS Technical Notes are designed to supplement the Bureau's regular publications program. They provide a means for making available scientific data that are of transient or limited interest. Technical Notes may be listed or referred to in the open literature.

For sale by the Superintendent of Documents, U.S. Government Printing Office, Washington, D.C., 20402.
(Order by SD Catalog No. C 13.46:555), Price 65 cents

CONTENTS

PAGE

1. Introduction and Highlights 1

2. Methods of Measurement for Semiconductor Materials

2.1 Resistivity 6

2.2 Carrier Lifetime 9

2.3 Inhomogeneities 12

2.4 Hall Effect 15

2.5 Specification of Germanium 15

2.6 References 20

3. Methods of Measurement for Semiconductor Process Control

3.1 Metallization Evaluation 22

3.2 Die Attachment Evaluation 25

3.3 Wire Bond Evaluation 27

3.4 Processing Facility 36

3.5 NASA Measurement Methods 40

3.6 References 40

4. Methods of Measurement for Semiconductor Devices

4.1 Thermal Properties of Devices 42

4.2 Thermographic Measurements 47

4.3 Microwave Device Measurements 47

4.4 Silicon Nuclear Radiation Detectors 50

4.5 Reference 53

Appendix A. Joint Program Staff 54

Appendix B. Committee Activities 55

Appendix C. Solid-State Technology and Fabrication Services . . . 57

Appendix D. Joint Program Publications 58

LIST OF FIGURES

PAGE

1. Resistivity profiles along a diameter of a thin, circular, *n*-type silicon wafer with a lapped surface obtained by the four-probe, photovoltaic, and two-probe methods 14

2. Resistivity profiles along a diameter of a thin, circular, *n*-type silicon wafer obtained by the four-probe and photovoltaic methods 14

3. Schematic illustration of the apparatus used in obtaining the infrared response of Ge(Li) detectors as a function of photon energy at 77 K 17

4. Infrared response of Ge(Li) Detector 88 as a function of incident photon energy at 77 K 18

5. Infrared response of Ge(Li) Detector 619 as a function of incident photon energy at 77 K 18

6. Interferograms of two diamond stylus tips 23

7. SEM photomicrographs of two diamond stylus tips showing contrasting surface features 23

8. Threshold adhesion failure loads for an aged aluminum film on a fused quartz substrate 24

9. Transient thermal response normalized to its steady state value as a function of the width of the applied power pulse . 26

10. Typical SEM photomicrographs (approximately 500X) of first bonds made with varying amounts of intentionally introduced work-stage motion 28

11. Placement of bonding tool on bond loop for ultrasonic vibration screening test. 32

12. Geometric parameters for the destructive, double-bond pull test 32

13. Dependence of T_{wt}/T and Θ_t for various ratios Θ_d to Θ_t. . . . 34

14. Photomicrograph of bipolar test chip. 37

15. Common emitter characteristic of *n-p-n* transistor in bipolar test chip 37

16. Detail of platinum-bonded, silicon-sandwich temperature sensor 39

17. Small-signal, reverse-voltage, transfer ratio characteristics for a medium power, triple-diffused, *n*-*p*-*n* silicon transistor.. 43

18. SEM photomicrographs (2000X) of thermographic phosphor particles of nominal 9-μm size.. 46

19. Detector noise (resulting from radiation damage) as a function of the fluence of 400-keV electrons incident on the (A) gold contact and (B) aluminum contact of a 1000-μm thick, silicon, surface-barrier detector 52

LIST OF TABLES

1. Silicon wafers used in current and probe loading study 6

2. Recommended values of current for four-probe resistivity measurements on silicon wafers 6

3. Filament lifetime by the PCD method 10

FOREWORD

The Joint Program on Methods of Measurement for Semiconductor Materials, Process Control, and Devices was undertaken in 1968 to focus NBS efforts to enhance the performance, interchangeability, and reliability of discrete semiconductor devices and integrated circuits through improvements in methods of measurement for use in specifying materials and devices and in control of device fabrication processes. These improvements are intended to lead to a set of measurement methods which have been carefully evaluated for technical adequacy, which are acceptable to both users and suppliers, and which can provide a common basis for the purchase specifications of government agencies. In addition, such methods will provide a basis for controlled improvements in essential device characteristics, such as uniformity of response to radiation effects.

The Program is supported by the National Bureau of Standards,[†] the National Aeronautics and Space Administration,[*] the Defense Atomic Support Agency,[×] the U. S. Navy Strategic Systems Project Office,[§] and the U. S. Naval Electronic Systems Command.[+] Because of the cooperative nature of the Program, there is not a one-to-one correspondence between the tasks described in this report and the projects by which the Program is supported. Although all sponsors subscribe to the need for the entire basic program for improvement of measurement methods for semiconductor materials, process control, and devices, the concern of certain sponsors with specific parts of the Program is taken into consideration in planning.

---

† Through Research and Technical Services Projects 4251120, 4251123, 4251126, 4252114, 4252128, 4254111, 4254112, and 4254115.

* Through Order ER-22448, Electronics Research Center. (NBS Project 4251523)

× Through Project Order 808-70. (NBS Project 4259522)

§ Administered by U. S. Naval Ammunition Depot, Crane, Indiana through Project Orders PO-0-0036 and PO-0-0055. (NBS Project 4259533)

\+ Through Project Order PO-0-0119. (NBS Project 4252534)

METHODS OF MEASUREMENT FOR SEMICONDUCTOR MATERIALS, PROCESS CONTROL, AND DEVICES

Quarterly Report
January 1 to March 31, 1970

This quarterly progress report, seventh of a series, describes NBS activities directed toward the development of methods of measurement for semiconductor materials, process control, and devices. Principal emphasis is placed on measurement of resistivity, carrier lifetime, and electrical inhomogeneities in semiconductor crystals; evaluation of wire bonds, metallization adhesion, and die attachment; and measurement of thermal properties of semiconductor devices and electrical properties of microwave devices. Work on related projects on silicon nuclear radiation detectors and specification of germanium for gamma-ray detectors is also described. Supplementary data concerning staff, standards committee activities, technical services, and publications are included as appendixes.

Key Words: Alpha-particle detectors; aluminum wire; carrier lifetime; die attachment; electrical properties; epitaxial silicon; gamma-ray detectors; germanium; gold-doped silicon; metallization; methods of measurement; microelectronics; microwave devices; nuclear radiation detectors; resistivity; semiconductor devices; semiconductor materials; semiconductor process control; silicon; thermal resistance; thermographic measurements; ultrasonic bonder; wire bonds.

1. INTRODUCTION AND HIGHLIGHTS

This is the seventh quarterly report to the sponsors of the Joint Program on Methods of Measurement for Semiconductor Materials, Process Control, and Devices. It summarizes work on a wide variety of measurement methods that are being studied at the National Bureau of Standards. Since the Program is a continuing one, the results and conclusions reported here are subject to modification and refinement.

Nearly twenty tasks, each directed toward a particular material or device property or measurement technique, have been identified as parts of the Program. The report is subdivided according to these tasks. Section 2 deals with tasks on methods of measurement for material; section 3, with those on methods of measurement for process control, and section 4, with

those on methods of measurement for devices. References for each section are listed in a separate subsection at the end of that section.

Besides the tasks sponsored under the Joint Program, this report contains descriptions of activity on related projects supported by NBS or other agencies. Although the specific objectives of these projects are different from those of the Joint Program, much of the activity undertaken in these projects will be of interest to Joint Program sponsors. The sponsor of each of these related projects is identified in the description of the project.

An important part of the work which generally falls outside the task structure is participation in the activities of various technical standardizing committees. The list of personnel involved with this work given in Appendix B suggests the extent of this participation.

The report for each task includes the long-term objective, a narrative description of progress made during this reporting period, and a listing of plans for the immediate future. Additional information concerning the material reported may be obtained directly from individual staff members connected with the task as indicated throughout the report. The organization of the Joint Program staff and telephone numbers are listed in Appendix A.

Background material on the Program and individual tasks may be found in earlier reports in this series as listed in Appendix D. From time to time, publications that describe some aspect of the program in greater detail are prepared. Current publications are also listed in Appendix D.

Following are highlights of the technical activity during this reporting period.

Resistivity — Study of the four-probe resistivity measurement technique is being continued. This study is seeking to improve understanding and control of the factors which limit the precision of the technique and to extend its range of applicability to specimens with higher resistivity, polished surfaces, or thin layers. Other effort has been directed toward consideration of various systems for automatically recording and analyzing the data from the four-probe measurements.

Investigation of the spreading resistance technique was limited to further attempts to reduce the noise level in the detection circuit. The automatic sequencing system for selecting bias voltages used in the capacitance-voltage technique was nearly completed. Renewed interest in obtaining silicon resistivity standards from NBS as expressed by various representatives of the industry resulted in further consideration of various methods for furnishing such standards.

Carrier Lifetime — A series of measurements to establish multi-operator, single-laboratory precision for the revised photoconductivity decay method for measuring minority carrier lifetime in bulk single crystals has been completed. Additional changes are being made in the wording of the procedure in order to improve its clarity before continuing with the second phase of the experiment. The analysis of the surface photovoltage method for measuring minority carrier lifetime in thin specimens was completed. It was found that this method cannot be used to obtain the diffusion length if the layer thickness is less than 1.2 times the diffusion length. A new circuit has been built for making diode recovery measurements. This circuit permits greater flexibility in the choice of magnitude of both forward and reverse currents. Near the end of the quarter the study of methods for measuring carrier lifetime in transistor structures was resumed.

Inhomogeneities — Some of the problems encountered in measuring photoconductivity near knife-edge pressure contacts have been resolved. Photovoltaic resistivity profiles have been made successfully on wafers with chemically-mechanically polished surfaces without contacting the polished surfaces. In a number of instances good agreement has been obtained between resistivity profiles measured with the photovoltaic technique and the two-probe technique. Efforts to quantify the agreement achieved are being considered.

Other Measurement Methods for Materials — Tests on the Hall effect apparatus, which had previously been modified to permit measurement of higher resistivity specimens, showed that measurements can be made on specimens with resistance up to 1 TΩ with a maximum response time of about 20 s. The apparatus appears to be satisfactory for measurements of Hall coefficient and resistivity on a wide variety of specimens including high-resistivity, gold-doped silicon. Electrical measurements on additional gold-doped silicon wafers were postponed until additional neutron activation analysis data can be obtained.

Metallization Evaluation — The surface tips of diamond styli employed in the scratch test were examined with an interferometer and a scanning electron microscope. It was found that the tips are neither spherical nor radially symmetric and that the surface texture can vary substantially from tip to tip. Additional studies designed to test the validity of the concept of threshold adhesion failure showed good consistency when measurements were made with a single scratching tip but wide variability when different tips were used.

Die Attachment Evaluation — Equipment for measuring thermal resistance and transient thermal response of diodes was designed. Procedures for attaching the diode chips to headers were established, but fabrication of completed devices was delayed because of continuing difficulties with scribing and breaking.

Wire Bond Evaluation — Experiments were undertaken to evaluate the significance of relative motion between work stage and transducer mount on the occasional lift-off or weak bond in a series of otherwise strong bonds. The bonding machine was subjected to intentional motion during the formation of ultrasonic wire bonds. Bonds were observed visually and with the scanning electron microscope. As the degree of motion increased, the bond deformation began to vary widely from bond to bond and lift-off bonds were produced more often than would be expected during a normal wire bonding operation.

Magnetic detectors were found to be well adapted to reestablishing tool tip vibration amplitude after changing tools or in retuning. These detectors are simpler and more rugged than the capacitor microphone and hence are well adapted for use in tuning ultrasonic wire bonding machines on production lines.

Preliminary investigations were carried out on a new bond screening test which consists of applying ultrasonic energy to each individual bond loop. In addition to screening for bond quality, the method appears to offer a means of assessing damage, if any, inflicted on a bond pair by prestressing or by other physical means of evaluating bond quality.

The first draft of the section on evaluation methods that will be included in the critical review is nearing completion. Detailed analyses of the destructive, double-bond pull test and the centrifuge test have been prepared. These analyses, which include the calculation of the relationships between the test stress and the resulting tensile stress along the wire, are summarized in this report.

Processing Facility — Procedures for producing a bipolar test slice, for chemically-mechanically polishing silicon wafers, and for using negative-working photoresists have been developed. Design, construction, and testing of the platinum-bonded, silicon-sandwich temperature sensor were completed.

NASA Measurement Methods — NASA measurement methods have been reviewed with emphasis on the correlation of the precision needed to meet the requirements for microcircuit line certification with the precision to be expected from the measurement methods. An extensive table that shows these correlations and equivalent ASTM tests where these are available has been prepared.

Thermal Properties of Devices — Difficulties in correlating measurements of thermal resistance of transistors under calibration and test conditions have been resolved with the addition of a cascade monostable multivibrator to the test circuit. The multivibrator delays the switching

time in the base current for a time sufficient to allow the collector switching transistor to turn off. Use of the multivibrator also eliminates the unstable condition that previously occurred whenever the total base current required to maintain a constant collector current was less than the base current used for measuring the emitter-base voltage.

Microwave Device Measurements — Activity in this area increased with the identification of needs and with the selection of parameters for initial investigation. Assembly of the X-band system for measuring mixer diode noise ratio and related quantities continued. A survey is being conducted to determine the problems encountered in the various techniques now being used to measure conversion loss in mixer diodes. Apparatus is being assembled to study methods for measuring mixer diode impedance and burn-out characteristics. A survey of microwave transistor measurement requirements is underway.

Meetings — Arrangements for the Symposium on Silicon Device Processing to be held in June, 1970, under the joint sponsorship of ASTM Committee F-1 and the National Bureau of Standards have been completed. The papers to be presented at the various sessions were selected at the February meeting of Committee F-1. The proceedings of the Symposium will be published as an NBS special publication.

The limited-attendance meeting for exchange of information on problems associated with ultrasonic wire bonds has been postponed. This action was in response to a directive from the requesting sponsor which cited the need to reduce travel expenses at this time.

2. METHODS OF MEASUREMENT FOR SEMICONDUCTOR MATERIALS

2.1 RESISTIVITY

Objective: To develop methods, suitable for use throughout the electronics industry, for measuring resistivity of bulk, epitaxial, and diffused silicon wafers.

Progress: Study of the four-probe resistivity measurement technique is being continued. This study is seeking to improve understanding and control of the factors which limit the precision and accuracy of the technique and to extend its range of applicability to specimens that have higher resistivity, polished surfaces, or thin layers. Several systems for automatically recording and analyzing data from the four-probe measurements have been considered. Investigation of the spreading resistance technique was limited to further attempts to reduce the noise level in the detection circuit. The automatic sequencing system for selecting bias voltages used in the capacitance-voltage technique was nearly completed. Renewed interest in obtaining silicon resistivity standards from NBS, as expressed by various representatives of the industry, resulted in further consideration of various methods for furnishing such standards.

Four-Probe Method — In the study of current and pressure dependence of resistivity as measured by the four-probe method, nearly all data has been obtained from wafers with lapped surfaces. Measurements were made on seven wafers with room temperature resistivities between 0.0009 and 120 Ω-cm (see Table 1). Based on preliminary analysis of this data,

Table 1 - Silicon wafers used in current and probe loading study

Specimen No.	Resistivity (Ω-cm)	Type
612522-2	0.000979[a]	*p*
600200-2	0.007763[a]	*p*
607075-2	0.10909[a]	*p*
325-2	1.085[b]	*p*
49445-2	11.869[a]	*p*
66969-1	113.06[a]	*p*
71983-2	101.08[a]	*n*

[a] Value of resistivity taken from ASTM round robins (see NBS Tech. Note 520, p. 6). Note that there are a number of typographical errors in Table I of NBS Tech. Note 520. A correction sheet is available.

[b] Average value for all measurements taken in the present study.

Table 2 - Recommended values of current for four-probe resistivity measurements on silicon wafers[a]

Resistivity (Ω-cm)	Current (mA)
< 0.012	100
0.008 to 0.6	10
0.4 to 60	1
40 to 1200	0.1
> 800	0.01

[a] Method of Test for Resistivity of Silicon Slices Using Four Pointed Probes (ASTM Designation: F84-68T), *1969 Book of ASTM Standards*, Part 8, November, 1969. This method permits a variation of ±20 percent of the nominal recommended value of current and a choice where two currents are given for the same resistivity.

several conclusions can be drawn. At current levels near the recommended values (see Table 2), the measured resistivity is nearly independent of the current, but large variations in the current produce noticeable changes in the measured value of resistivity.

For low currents, 0.1 times the recommended value, the measured value of resistivity tends to be low by about 1 percent. In addition, the data at this low current level exhibits much more scatter than at the other current levels. This is probably due to a decreased signal-to-noise ratio at these low signal levels.

At currents ten times the recommended value the measured value tends to be high by about 1 percent. For all wafers with resistivity below 10 Ω-cm a temperature increase at the probes as high as 15 deg C was observed with an infrared radiometric microscope. The associated temperature corrections are sufficient to remove the current dependence only for the 0.001 and 0.01 Ω-cm specimens; for the 0.1 and 1 Ω-cm specimens the temperature corrections are too large and for specimens 10 Ω-cm and higher no temperature change was observed. In addition to the heating effects in low resistivity wafers, there may be injection effects in all wafers; neither effect has been characterized sufficiently to develop suitable correction factors for use at these high current levels.

It seems clear that measurement at the extremes of current levels used in this study should be avoided. It was observed that for measurements on specimens 10 Ω-cm or greater, a current level of three times the recommended value resulted in distinctly less dependence of measured resistivity upon probe loading and less scatter of data at any single load than did other current levels.

For most specimens a probe loading of 150 g resulted in less dependence of measured resistivity upon current level than did the other probe loads used: 100, 50, and 25 g. However at any given current level, use of a 150 g probe load frequently resulted in more scatter of the data than did use of the lighter probe loads. This effect, which became more pronounced with time, appears to be directly related to the cumulative destructive effects of high probe pressure and high currents on the probe material.

A new four-probe resistivity circuit which includes additional capabilities for measuring conductivity type [1] and probe-to-wafer contact resistance is being built. Various systems for automatically recording and analyzing data from four-probe measurements are being investigated. Possible systems for such applications include an on-site computer system, a remote time-sharing computer, or a data recording system used in conjunction with batch processing on the NBS computer facility. Need for nearly real-time reduction of data is the prime factor to be considered.

This essentially restricts the choice to the first two possibilities.
(F. H. Brewer, D. R. Ricks, and J. R. Ehrstein)

Round-Robin Experiments — Two round-robin tests for the four-probe method are being coordinated in conjunction with ASTM Committee F-1. Three new specimens were obtained for use in the first which involves measurement of resistivity of silicon epitaxial layers deposited on substrates of the opposite conductivity type. A total of six wafers and three analog resistor circuits was sent to the first participant in this round robin. He has completed his measurements and sent the specimens to the next of the nine additional laboratories scheduled to participate in this round robin.

Three of the nine groups participating in the four-probe high-resistivity silicon wafer round robin have completed their measurements. No data have been received from participants in either round robin.
(F. H. Brewer)

Silicon Resistivity Standards — Renewed interest in obtaining silicon resistivity standards from NBS has been expressed by representatives of various industrial organizations. One means for supplying such standards is an extended collaborative reference program in which various interested laboratories would participate on a fee-charged basis with NBS [2]. In a program such as this, specimens characterized at NBS are sent to a participating laboratory for measurement and then returned to NBS for characterization again before being sent to another participating laboratory. Each laboratory receives an up-to-date record of the multi-laboratory measured value for each specimen and the relationship between its measured value and the multi-laboratory value. In this type of program, each laboratory can expect to receive specimens for measurement several times each year. (J. R. Ehrstein and W. M. Bullis)

Capacitance-Voltage Method — A phase-locked detection system was considered for making the capacitance-voltage measurements. It was expected that such a system would allow capacitance measurements to be made over a wider range of measurement frequency than would otherwise be possible. However, difficulties in design which resulted in degradation of accuracy for low-Q capacitors led to postponement of further effort on this aspect of the measurement. Assembly of the fully automatic sequencing system for selection of the bias voltage in the capacitance-voltage measurement is continuing. Measurements on both planar and mesa diodes fabricated on bulk silicon wafers were deferred pending completion of the apparatus.
(G. N. Stenbakken)

Plans: Work on the dependence of four-probe resistivity measurements on current and probe force will proceed on mechanically-polished surfaces of the same wafers which have been already measured with lapped surfaces.

The modified four-probe measurement circuit will be completed. An automatic data acquisition system for four-probe measurements will be obtained and placed into operation.

Capacitance-voltage measurements will be made on planar diodes to evaluate the important parameters to be controlled in this type of measurement.

A standard four-probe assembly will be used with a load of 20 to 50 g to make spreading resistance measurements in order to gain further understanding of the sources of electrical noise in the system. Measurements will be made with two- and three-probe configurations. Measurements will then be undertaken to determine the effect on measurement precision of probe material (osmium and tungsten carbide), specimen surface condition (lapped and mechanically polished) for silicon wafers in the 0.1 to 10 Ω-cm resistivity range.

The extent of industry interest in silicon resistivity standards will be explored further.

2.2 CARRIER LIFETIME

Objective: To determine the fundamental limitations on the precision and applicability of the photoconductive decay method for measuring minority carrier lifetime and to develop other methods for measuring minority carrier lifetime in germanium and silicon which are more precise, more convenient, and more meaningful in the specification of material for device purposes.

Progress: A series of measurements to establish a single-laboratory precision for the revised photoconductive decay (PCD) method for measuring minority carrier lifetime in bulk single crystals has been completed. Additional changes are being made in the wording of the procedure in order to improve its clarity before continuing with the second phase of the experiment. The analysis of the surface photovoltage (SPV) method for measuring minority carrier lifetime in thin specimens was completed. It was found that this method cannot be used to obtain the diffusion length if the layer thickness is less than 1.2 times the diffusion length. A new circuit has been built for making diode recovery measurements. This circuit permits greater flexibility in the choice of magnitude of both forward and reverse currents. Near the end of the quarter the study of methods for measuring carrier lifetime in transistor structures was resumed.

Bulk Crystals — The experiment to establish a multi-operator, single-laboratory precision for the revised procedure (NBS Tech. Note 520, p. 14) was continued. In the first phase, measurements of photoconductive decay

Table 3. Filament Lifetime by the PCD Method

Operator \ Specimen		SS11 n-Ge 8 Ω-cm	16444/2 p-Si 1500 Ω-cm	SS6 p-Si 270 Ω-cm	SS10 n-Ge 8 Ω-cm	SS12 n-Ge 8 Ω-cm
A	$\bar{\tau}_f$, μs	87.44	1312.	27.50	288.2	46.75
	s, μs	1.34	19.	0.61	1.9	0.40
	s, %	1.5	1.5	2.2	0.65	0.84
B	$\bar{\tau}_f$, μs	86.15	1400.	30.80	282.3	52.90
	s, μs	5.02	16.	0.86	11.7	0.94
	s, %	5.8	1.2	2.8	4.2	1.8
C	$\bar{\tau}_f$, μs	90.25	1331.	24.31	269.4	42.35
	s, μs	0.64	15.	0.12	2.0	0.33
	s, %	0.71	1.1	0.48	0.76	0.78
D	$\bar{\tau}_f$, μs	83.12[a]	1256.[b]			
	s, μs	0.53	49.			
	s, %	0.64	3.9			
E	$\bar{\tau}_f$, μs	88.82				
	s, μs	1.31				
	s, %	1.5				
F	$\bar{\tau}_f$, μs	87.83				
	s, μs	2.54				
	s, %	2.9				
Grand average	$\bar{\tau}_f$, μs	87.7[a]	1330.[b]	27.5	280.	47.3
Sample standard deviation	s, μs	3.0	57.	2.8	10.4	4.5
Two relative sample standard deviations	R2S%	6.9	8.6	20.	7.4	19.

a Three readings of operator D were rejected and are not included in these figures.
b One reading of operator D was rejected and is not included in these figures.

time were made on five of the eight specimens selected for this experiment. Each of these specimens was measured five times by two to six operators with results as summarized in Table 3. Bulk lifetimes were calculated from the average measured filament lifetime, τ_f. In each case the relative sample standard deviation for the calculated bulk lifetime was larger than that obtained for τ_f. During the course of these measurements, a number of suggestions for improvements in the form and content of the procedure were made. These are being incorporated in the text before beginning a second series of measurements. A summary of the experimental work which led to the revisions in the PCD procedure is being prepared for publication.. (R. L. Mattis)

SPV measurements of carrier lifetime in bulk crystals were repeated on a number of specimens that had been previously measured both by the PCD and SPV methods. These measurements were repeated in an attempt to determine the causes of differences between values obtained by the PCD and SPV methods. The results indicate that the SPV measurements are more variable than was expected, and that this variability is likely to cause the observed differences. The origin of the variability has not yet been determined.

Epitaxial Layers — Extension of the analysis of the SPV method for measuring minority carrier lifetime to thin specimens such as epitaxial layers was completed. The photon intensity required to produce a given SPV response for a particular wavelength was linearly related to the reciprocal absorption coefficient at that wavelength. This results in a straight-line plot which can be extrapolated to zero photon intensity. For layer thicknesses greater than six diffusion lengths the magnitude of this intercept is equal to the diffusion length. The intercept for layer thickness less than 1.2 diffusion lengths but greater than the surface depletion depth is independent of the diffusion length. For this case if it is assumed that the boundary between the epitaxial layer and the substrate is abrupt and that this boundary is an infinite sink for excess carriers the magnitude of the intercept is one-third the layer thickness. If the same assumptions are made, it is possible to deduce the approximate diffusion length from a knowledge of the layer thickness and the measured intercept value for layer thicknesses between 1.2 and 6 diffusion lengths. Details of this analysis are being prepared for publication. (W. E. Phillips)

Inquiries to several representatives of the semiconductor device industry revealed considerable interest in the measurement of carrier lifetime in epitaxial layers by the metal-oxide-semiconductor (MOS) capacitance method. At least three organizations are working actively in this area. Each using a somewhat different approach to extract the carrier lifetime from experimental data. An analysis of the various methods reported in the literature (NBS Tech. Note 527, pp. 9-10) was begun in order to determine the extent of their equivalence. (R. L. Mattis)

Diodes — A new circuit for reverse recovery measurements was designed and built. This circuit allows wide flexibility and a choice of magnitude for both forward and reverse currents. Initial tests indicate that better agreement between the values of lifetime measured by the reverse recovery technique and the voltage decay technique can be obtained. (A. J. Baroody)

Plans: After the revision of the procedure, a second series of measurements to establish a multi-operator, single-laboratory precision for the measurement of carrier lifetime by the PCD method will be initiated. Preparation of the summary report on the PCD method will continue. Additional SPV measurements of carrier lifetime in bulk crystals will be made in an effort to identify the sources of variability.

The analysis of the various forms of the MOS capacitance method for measuring carrier lifetime in epitaxial layers will be continued. Consideration of the applicability of this measurement technique to specimens with layer thickness comparable to or shorter than the diffusion length will begin.

Further experimental studies aimed at resolving the discrepancy between the reverse recovery technique and the voltage decay technique will be conducted. Both low-current and high current transition limits for the reverse recovery technique will be studied experimentally. Dependence of the measured values of carrier lifetime on frequency and current magnitude for both techniques will be studied.

Review and study of methods for measuring carrier lifetime in transistor structures will continue.

2.3 INHOMOGENEITIES

Objective: To develop improved methods for measuring inhomogeneities responsible for reducing performance and reliability of germanium and silicon devices and, in particular, to evaluate a photovoltaic method as a means for measuring radial resistivity gradients in germanium and silicon circular wafers.

Progress: Three comparative studies were undertaken in the continuing investigation of the relationship between photovoltage and radial resistivity gradients in thin, circular wafers.

A comparison of the photovoltage signal as measured with small semicircular contacts at the ends of the measurement diameter and with similarly located knife-edge contacts indicated that similarly shaped profiles were obtained. The dependence of the photoconductivity on the polarity of

the current through the specimen when knife-edge contacts are used was also investigated. If a voltage is applied to the knife-edge contacts, one behaves as a reverse-biased junction, the other as a forward-biased junction. It was found that the profiles are the same for both directions of the current in the central region of the wafer, but as the light probe approaches one of the contacts the apparent photoconductivity signal is much larger when the contact is reverse biased than when it is forward biased. A correct indication of the photoconductive signal is apparently obtained if data taken near reverse-biased contacts are ignored since the photoconductive signal near forward-biased contacts agrees with that obtained with the ohmic semi-circular contacts.

Comparative two-probe, four-probe, and photovoltaic measurements were made on a specimen with an asymmetrical gradient. The photovoltaic measurement was made with knife-edge pressure contacts. The results, shown in Fig. 1, indicate that the agreement between the photovoltaic and two-probe methods is substantially better than that between either of these and the four-probe method. This serves to confirm the difficulty in spatial resolution encountered when the four-probe method is applied to the measurement of resistivity gradients (NBS Tech. Note 520, p. 17).

A preliminary investigation of the applicability of the photovoltaic technique to measuring resistivity gradients on thin, circular wafers with polished surfaces was undertaken on a wafer with a very long bulk lifetime. In such a wafer, the effective lifetime is significantly influenced by surface recombination. Photovoltaic measurements were made on the wafer first with lapped surface and then after the surface had been chemically-mechanically polished. The photovoltage was increased, after polishing, by a factor of four which suggests that the effective carrier lifetime was increased substantially. No increase in the influence of contacts was noted, but the relatively large photovoltage due to the resistivity gradient in the vicinity of the contacts may have masked contact effects. The resistivity profiles obtained from these measurements are shown in Fig. 2.

Use of the knife-edge contacts permits measurements of the specimen resistivity by the van der Pauw method [1]. In all instances the van der Pauw technique has yielded an average resistivity value which lies within the range of resistivity as measured by the two-probe or four-probe techniques. (D. L. Blackburn)

<u>Plans</u>: To obtain additional information concerning the extent of correlation between two-probe and photovoltaic measurements, two-probe resistivity profiles will be measured on bars from several wafers on which photovoltaic and four-probe resistivity profiles have already been completed. Efforts to obtain a quantitative measure of correlation between the two techniques will be made. A series of experiments designed to gain statistical confidence in the measured correlations will be initiated.

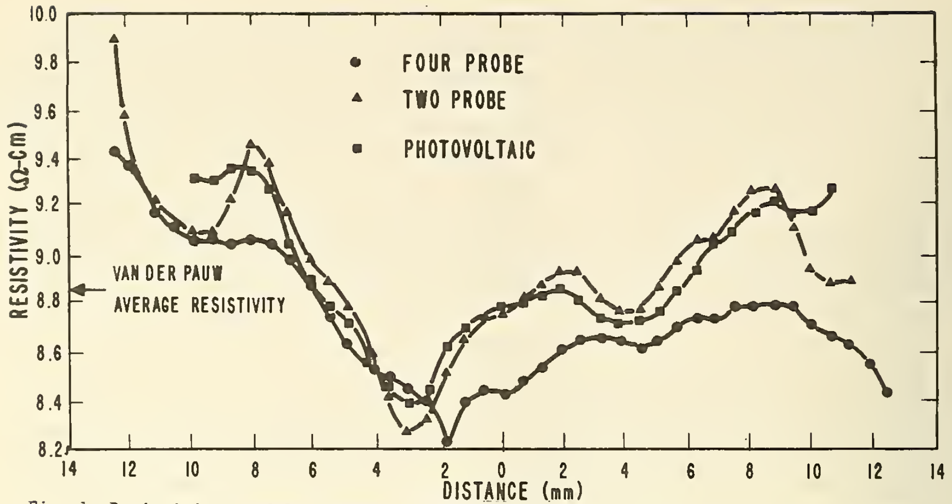

Fig. 1 Resistivity profiles along a diameter of a thin, circular, *n*-type silicon wafer with a lapped surface obtained by the four-probe, photovoltaic, and two-probe methods. The wafer diameter is 28 mm.

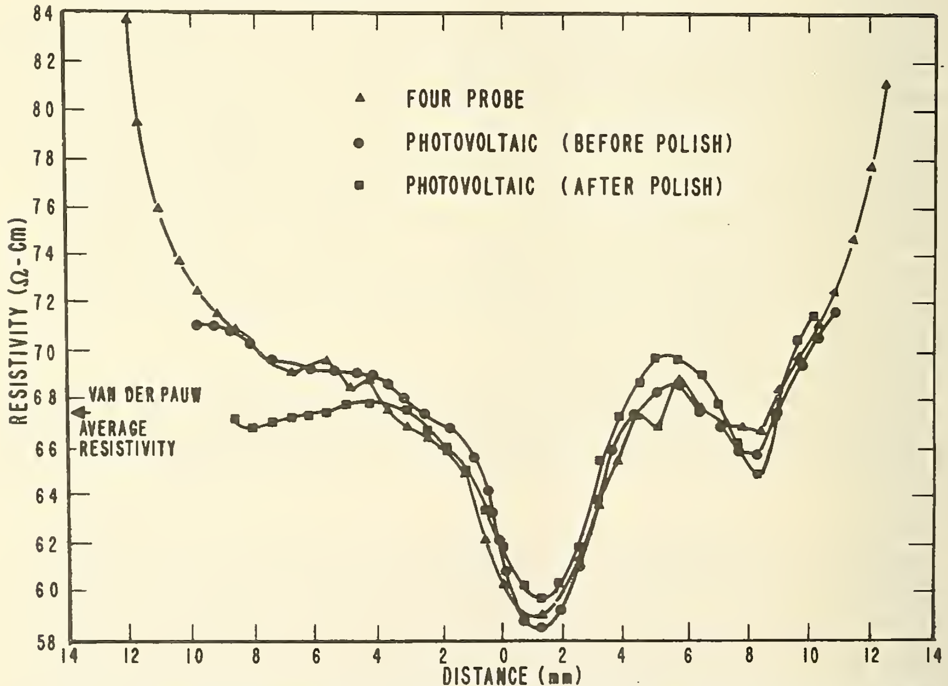

Fig. 2 Resistivity profiles along a diameter of a thin, circular, *n*-type silicon wafer obtained by the four-probe and photovoltaic methods. The four-probe measurement was made on a lapped surface. Photovoltaic measurements were made both on the lapped surface and on the same surface after it was chemically-mechanically polished. The wafer diameter is 28 mm.

Preparation will begin on a report describing in detail the results of work on this method.

2.4 HALL EFFECT

Objective: To establish a facility for making measurements of Hall coefficient as a function of temperature between 4 and 350 K and to improve methods for collecting and interpreting Hall-effect data.

Progress: The accuracy with which measurements can be made on high resistance specimens was determined for the modified Hall-effect apparatus. For a 0.5 TΩ resistor, the resistance value measured with the modified apparatus was within 1 percent of the resistance value determined by direct measurement with a vacuum-tube electrometer. This result indicates that the electrical leakage is sufficiently low to allow measurements on specimens with resistance up to 1 TΩ. In an actual Hall specimen, additional resistance is present in the voltage leads. To simulate this situation, the potential drop across a 0.5 TΩ resistor was measured with a 1 TΩ resistor in one of the voltage leads. The value of the potential drop determined under these conditions differed by less than 0.5 percent from the value determined without the 1 TΩ resistor.

A germanium resistance thermometer, which yields improved temperature resolution at low temperatures, was installed in the Hall specimen holder. (W. R. Thurber)

Resumption of work on the report concerning Hall-effect measurements and their interpretation was again delayed. (W. M. Bullis)

Plans: The principal remaining phase of this task is the completion of the report concerning Hall-effect measurements and their interpretation. Work on this report will be resumed as soon as time permits. Hall-effect measurements will be made on gold-doped silicon wafers as these are prepared.

2.5 SPECIFICATION OF GERMANIUM†

Objective: To measure the properties of germanium crystals and to correlate these properties with the performance of germanium gamma-ray detectors in order to develop methods for the early identification of crystals suitable for fabrication into lithium-compensated gamma-ray detectors.

† Supported by the Division of Biology and Medicine, U. S. Atomic Energy Commission. (NBS Project 4259425)

Progress: Infrared response measurements have been completed on Ge(Li) detectors fabricated from two different germanium crystals. Preliminary analysis indicated that each of the two crystals exhibits infrared response characteristics typical of two types previously reported, however, certain spectral features have been seen for the first time. In other phases of the work, manuscripts for several reports are in various stages of completion, and two standard procedures are being prepared in cooperation with technical standardizing committees.

Characterization of Germanium — A draft of the text to accompany the six nomographs applicable to the fabrication and testing of Ge(Li) detectors has been prepared and is undergoing preliminary review.
(A. H. Sher)

A preliminary analysis of the results of measurements of oxygen concentration in germanium crystals by the methods of lithium mobility [1], lithium precipitation, and infrared absorption [2] has been completed. Excellent correlation was obtained among the three methods on 15 crystals with oxygen concentrations between 10^{13} and 10^{15} atoms/cm^3. While the infrared absorption technique can be used for oxygen analysis to a lower limit of about 10^{14} atoms/cm^3 the other two methods appear to be useful down to about 10^{13} atoms/cm^3 with the least ambiguous results being obtained by means of measurement of lithium mobility.
(A. H. Sher, W. K. Croll, and W. R. Thurber)

A report [3] has been prepared which compares four experimental infrared techniques involving both absolute and differential procedures and identifies sources of errors in the measurements. A report is also being prepared on the use of low temperature photoconductivity for identifying deep-lying impurities and determining their concentration in germanium and silicon. (W. R. Thurber)

Ge(Li) Detector Measurements — Infrared response (IRR) measurements were made on lithium-drifted, gamma-ray detectors fabricated from two different crystals. The IRR of detectors is being studied to determine whether this measurement can be used to identify crystals from which high quality gamma-ray detectors can be fabricated. The present experiments were intended to test the apparatus and to confirm results previously reported by Armantrout [4-7]. The spectra obtained were in general agreement with these results. The use of a higher resolution monochromator disclosed several spectral features not previously seen, but the importance of these features has not yet been determined.

In the IRR measurement, photons incident on a reverse-biased Ge(Li) detector induce the formation of free carriers in the depleted region of the device by excitation of carriers into or out of the energy levels

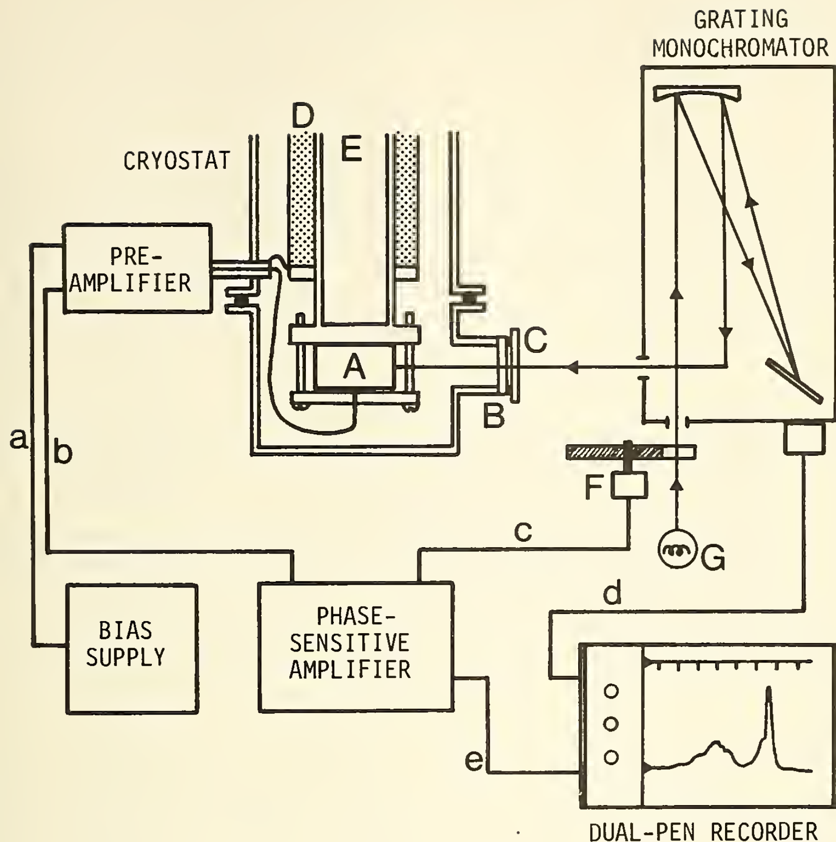

A - Ge(Li) DETECTOR
B - SAPPHIRE WINDOW, 2-mm THICK
C - GERMANIUM FILTER, 4-mm THICK
D - MOLECULAR SIEVE
E - LIQUID NITROGEN
F - LIGHT CHOPPER
G - LIGHT SOURCE

a - DETECTOR BIAS
b - DETECTOR RESPONSE SIGNAL
c - REFERENCE SIGNAL (13 Hz)
d - ENERGY-MARKER SIGNAL
e - DETECTOR RESPONSE SIGNAL

Fig. 3 Schematic illustration of the apparatus used in obtaining the infrared response of Ge(Li) detectors as a function of photon energy at 77 K.

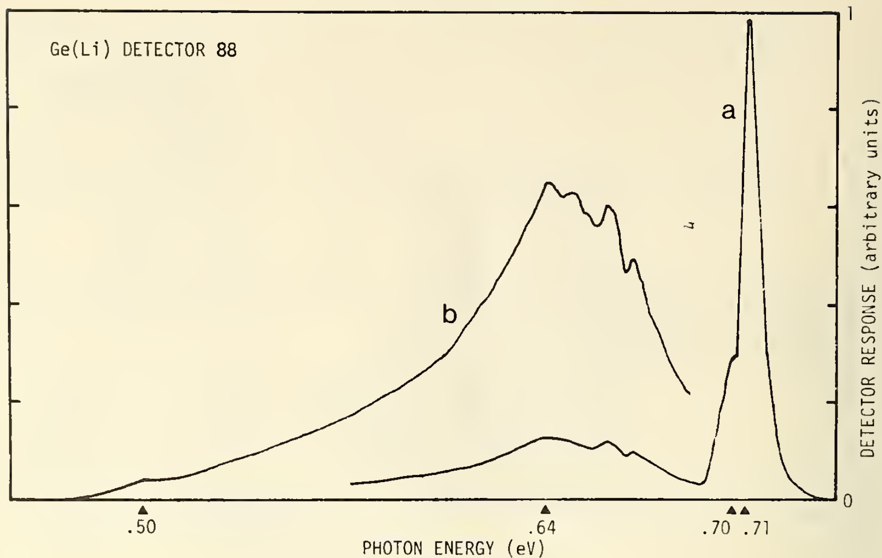

Fig. 4 Infrared response of Ge(Li) Detector 88 as a function of incident photon energy at 77 K. Curve b was obtained at a signal sensitivity increased above that for curve a by a factor of 5.

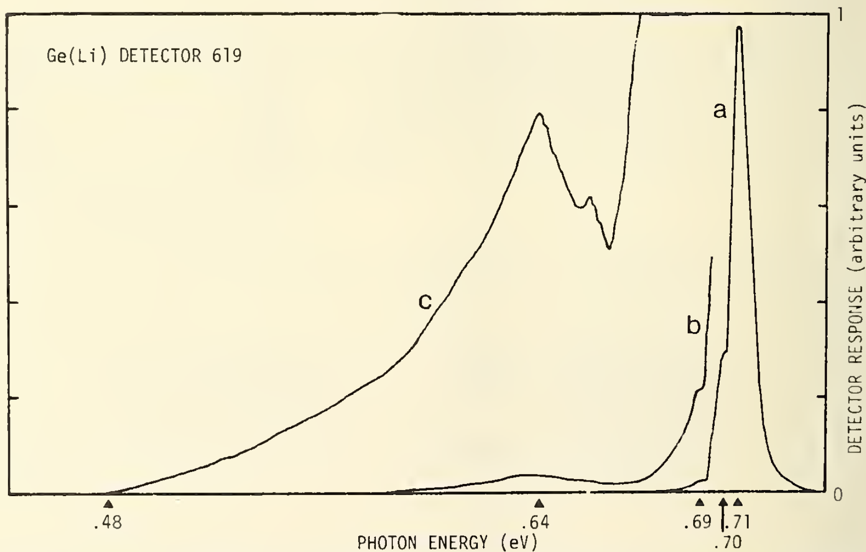

Fig. 5 Infrared response of Ge(Li) Detector 619 as a function of incident photon energy at 77 K. Curves b and c were obtained at signal sensitivities increased above that for curve a by factors of 10 and 40, respectively.

within the band gap. These levels are assumed to be caused by unwanted impurities in the crystal or by crystalline defects. The current due to the generation of free carriers and the subsequent transport of these carriers to the electrodes of the detector is measured as a function of the incident photon energy.

The apparatus for IRR measurements is shown in Fig. 3. The use of the grating monochromator and the phase-sensitive amplification system results in better energy resolution and a signal-to-noise ratio significantly improved over the equipment used for previous measurements [4-7]. The germanium filter was included because one was used by Armantrout [4-7]; it was used initially to facilitate comparison of the results with the earlier work. Since the germanium filter contributes significantly to the shape of the observed spectrum [8], its continued use is not planned.

Armantrout was able to categorize the IRR detector response into six distinct types [4-7]. Two of these types of response were observed. On Ge(Li) Detector 88, a "lithium-defect complex" was observed as shown in Fig. 4. There is a discrete level near 0.50 eV with a gradually increasing intensity to about 0.64 eV. The level near 0.70 eV and structure in the peak near 0.64 eV were observed for the first time. These features were reproducibly obtained, but it is not possible to interpret their importance at this stage of the analysis. The presence of a "lithium-defect complex" is expected to cause trapping of electrons in the detector [4-7]. Trapping was observed by irradiating Ge(Li) Detector 88 between the junction boundaries with a well-collimated beam of gamma rays.

"Lithium precipitates" formed within the compensated region of the detector were observed with Ge(Li) Detector 619. The general features of this type of response, shown in Curve a of Fig. 5 are similar to those reported previously [5]. However, use of increased signal sensitivity, depicted in Curves b and c, exposes additional structure. As in the case of Ge(Li) Detector 88, a peak in the main response occurs at 0.64 eV, and the response does not increase uninterruptedly into the band-edge peak. The appearance of a level at about 0.69 eV is also previously unreported. Collimated gamma-ray measurements on Ge(Li) Detector 619 confirmed the trapping of holes which is expected from the "lithium precipitates" [4-7].

Standardization Activities — Data submitted by four laboratories in the round-robin measurements of lithium-ion drift mobility which is being conducted by the Germanium Section of ASTM Committee F-1 have been analyzed [1]. Mean values of mobility, at 23.8°C, obtained on the two crystals studied were 2.13×10^{-10} and 2.56×10^{-10} $cm^2/V\text{-}s$ with estimated standard deviations of 13 and 10 percent, respectively. On the basis of these results, the test method is being prepared for committee ballot.

(A. H. Sher)

The first draft of a series of test procedures for the purposes of evaluation and comparison of lithium-drifted, germanium gamma-ray detectors has been prepared for the IEEE Nuclear Instruments and Detectors Committee. These testing procedures are intended to supplement a recently released ANSI/IEEE standard [9]. (A. H. Sher and J. A. Coleman)

Bibliography — Most of the references collected for inclusion in a bibliography on lithium-drifted germanium detectors have been entered on computer cards. This bibliography covers papers published after January 1, 1969 [10]. (A. H. Sher and H. E. Dyson)

Plans: Lithium mobility studies, detector performance measurements, and the correlation of etch-pit distributions on *p*-type germanium crystals with infrared response and with lithium driftability studies will continue. Further work on the IRR technique will continue with emphasis on the new features of the spectra reported above. IRR measurements will be made without the use of a germanium filter. Low-temperature impurity photoconductivity measurements will be deferred pending the outcome of the IRR measurements. Reports on the measurement of oxygen in germanium crystals and on the nomographs for the use in detector fabrication will be prepared as Technical Notes. Work on the bibliography will be continued and a review of diagnostic and evaluation techniques for the characterization of germanium for lithium-drifted, gamma-ray detectors will be prepared.

2.6 REFERENCES

2.1 Resistivity

1. W. A. Keenan, C. P. Schneider, C. A. Pillus; "TYPE-ALL System for Determining Semiconductor Conductivity Type," *Solid State Tech.* (to be published).

2. This concept is based on a successful collaborative reference program on paper testing established by NBS at the request of the Technical Association of the Pulp and Paper Industry, see *Nat. Bur. Stand. (U. S.), Tech. News Bull.* 53, 109 (1969).

2.3 Inhomogeneities

L. J. van der Pauw, "A Method of Measuring Specific Resistivity and Hall Effect of Discs of Arbitrary Shape," *Philips Research Reports* 13, 1-9 (1958).

2.5 Specification of Germanium

1. A. H. Sher, "Lithium-Ion Drift Mobility in Germanium," *J. Appl. Phys.* 40, 2600-2607 (1969).

2. R. J. Fox, "Lithium Drift Rate and Oxygen Concentration in Germanium," *IEEE Trans. Nucl. Sci.* NS-13, No. 3, 367-369 (1966).

3. W. R. Thurber, "Determination of Oxygen Concentration in Silicon and Germanium by Infrared Absorption," NBS Tech. Note 529, May, 1970.

4. G. A. Armantrout, "A Highly Sensitive Photoresponse Technique for Determining Impurity and Defect Energies and Concentrations in Germanium," UCRL-71625 (July 17, 1969).

5. G. A. Armantrout, "Trapping and Tailing Effects in Ge(Li) Detectors," Ph.D. Thesis, UCRL-50485 (August, 1969).

6. G. A. Armantrout, "Defect Study and Identification in Ge(Li) P-N Junction Radiation Detectors," *Metallurgical Trans.* 1, 659-665 (1970).

7. G. A. Armantrout, "Infrared Evaluation Techniques for Ge(Li) Detectors," *IEEE Trans. Nucl. Sci.* NS-17, No. 2, 16-23 (1970).

8. W. Kaiser, R. J. Collins, and H. Y. Fan, "Infrared Absorption in p-Type Germanium," *Phys. Rev.* 91, 1380-1381 (1953).

9. "USA Standard and IEEE Test Procedure for Semiconductor Radiation Detectors (For Ionizing Radiation)," USAS N42.1/IEEE No. 300 (February 19, 1969); published in *IEEE Trans. Nucl. Sci.* NS-16, No. 6, 271-282 (1969).

10. This bibliography is intended to supplement J. M. McKenzie, *Index to the Literature of Semiconductor Detectors*, Nat. Acad. Sci., Washington, D. C., 1969, which covers the period up to February, 1969. This index is available from the Printing and Publishing Office, National Academy of Sciences, 2101 Constitution Ave., Washington, D. C. 20418.

3. METHODS OF MEASUREMENT FOR SEMICONDUCTOR PROCESS CONTROL

3.1 METALLIZATION EVALUATION

Objective: To improve methods for measuring the properties of thin metal films with initial emphasis on adhesion of aluminum metallization deposited on various substrates.

Progress: The surface tips of diamond styli employed in the scratch test were investigated in detail, and the concept of threshold adhesion failure was developed further.

The modified shadowgraph technique (NBS Tech. Note 527, p. 25), in which a photograph of the silhouette of the stylus tip is matched to circles of known radius, has been found to be quite satisfactory for an overall representative measurement of tip radius. However, it cannot give any detailed information about the curvature and surface characteristics of the 0.5-μm wide portion of the tip which comes in contact with the metal film during scratching. By resting an optically flat microscope cover glass on the tip of a diamond stylus it is possible to generate interference figures which provide a contour map of the stylus tip. Typical interference patterns for two stylus tips with a nominal radius of curvature of 45 μm are shown in Fig. 6. The figure shows that the stylus tips are neither spherical nor radially symmetric. If circular cross sections are assumed for the case of stylus 2 (Fig. 6b), tip radii varying from 15 to 50 μm can be calculated.

Scanning electron microscope photomicrographs of the tips of two different diamond styli are shown in Fig. 7. The smoother of the two appears quite polished but with pits while the other has a "lemon peel" type of surface. These observations of surface characteristics and the nonuniformity of the tip radius lead one to expect that each stylus may show individual scribing and testing behavior.

This is confirmed by scratch tests. As an example, the two diamond styli shown in Fig. 6 were used to test the adhesion of a fully-aged, highly adherent aluminum film on a quartz substrate. The results of an up-and-down experiment in which alternate scratches were made by each stylus are shown in Fig. 8. It is quite clear that although each individual test results in the determination of a mean threshold failure load with very narrow spread, the two styli yield markedly different mean threshold failure loads.

Plans: Additional study of the determination of radius of curvature of stylus tips by interferometry will be undertaken in conjunction with investigations by the scanning electron microscope. The possibility of obtaining diamond styli with smoother surface finish will be explored.

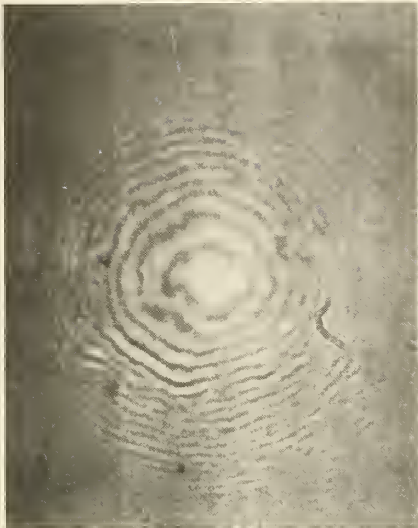

a: Stylus 1.

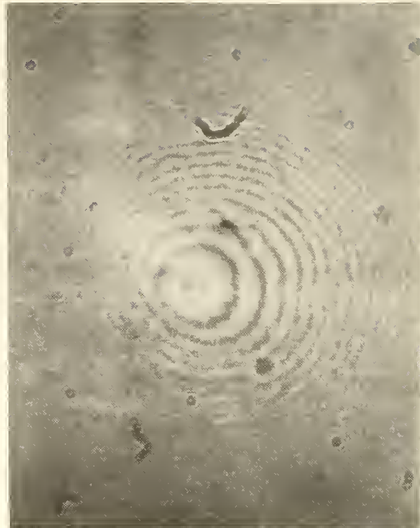

b: Stylus 2.

Fig. 6 Interferograms of two diamond stylus tips. Both styli have a nominal tip radius of 45 μm. Photographed with mercury green line (λ = 546.1 nm) at 1684X (a) and 1725X (b).

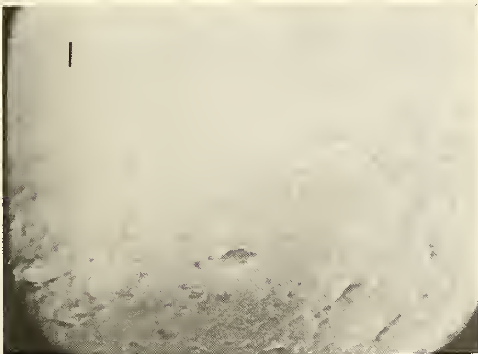

a: Nominal tip radius: 15 μm.
Magnification: 3800X.

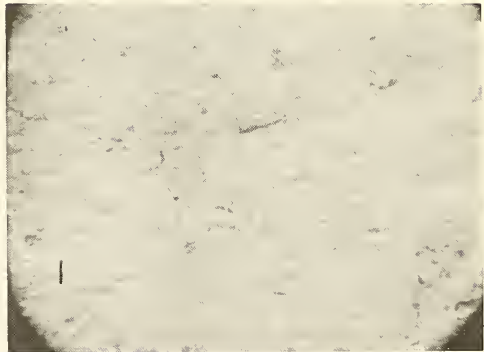

b: Nominal tip radius: 75 μm.
Magnification: 3600X.

Fig. 7 SEM photomicrographs of two diamond stylus tips showing contrasting surface features. The bar on each photomicrograph represents 1 μm.

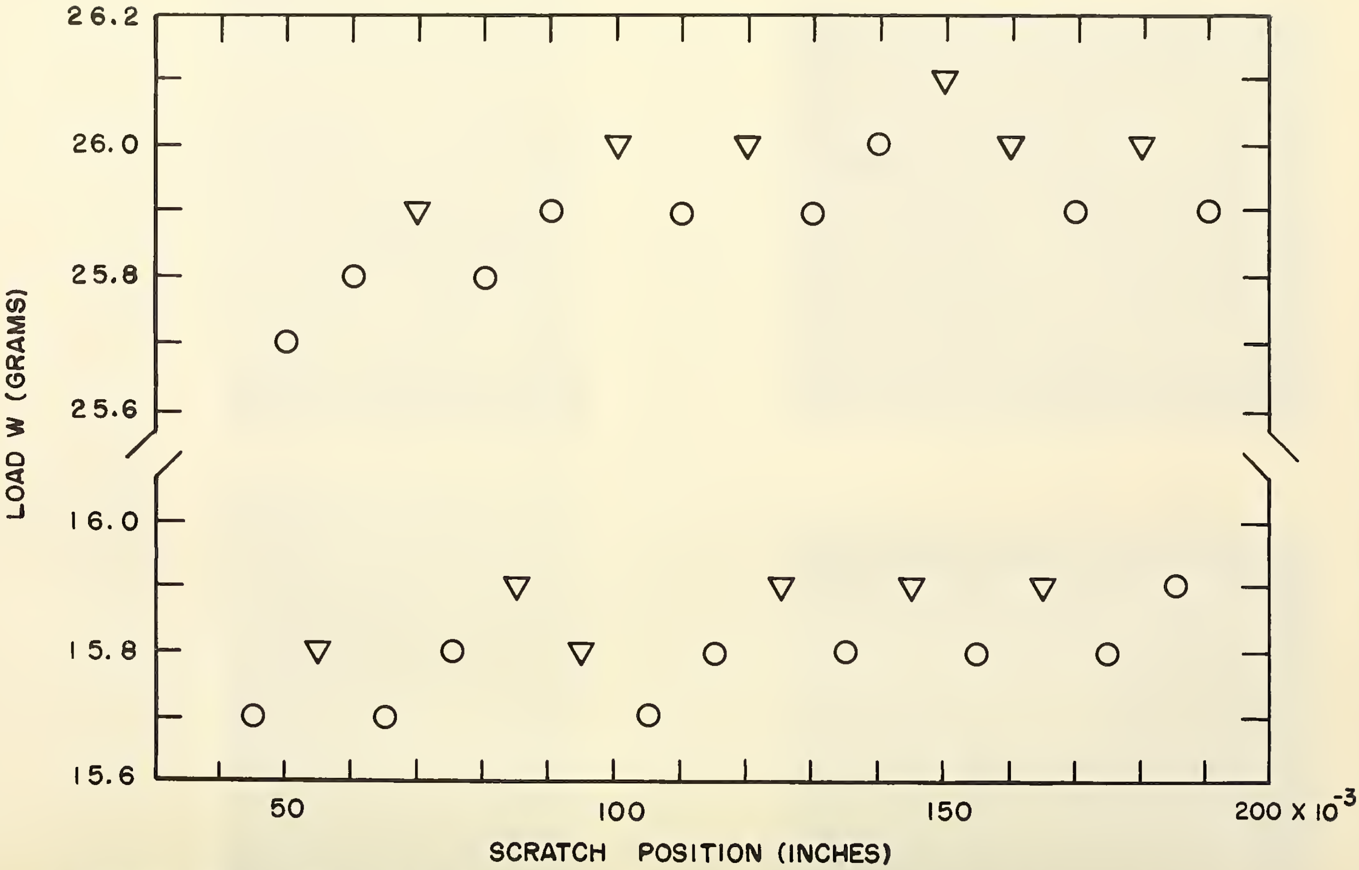

Fig. 8 Threshold adhesion failure loads for an aged aluminum film on a fused quartz substrate. Measurements were made with both diamond styli shown in Fig. 6. Failure occured at loads indicated by ∇, failure was not observed at loads indicated by o. For stylus 1 (lower plot), the average threshold failure load, $\bar{W}$ is 15.82 ± .04 g, while for stylus 2 (upper plot), $\bar{W}$ is 25.95 ± .06 g.

Additional scratch test measurements will be made on aluminum films deposited on quartz substrates in order to evaluate further the threshold adhesion failure concept. Both aged and freshly deposited films will be studied.

The literature search on adhesion testing will be continued as planned.

3.2 DIE ATTACHMENT EVALUATION

Objective: To evaluate methods for detecting poor die attachment in semiconductor devices with initial emphasis on the determination of the applicability of thermal measurements to this problem.

Progress: Because poor adhesion can impede the flow of heat from the chip to the case both the thermal resistance, R_Θ, and transient thermal response* of diodes are sensitive to the presence of voids. The technique selected for the measurement of these required thermal characteristics is based on a method proposed by Lockett, Bell, and Priston [1]. This method makes use of techniques commonly used to measure R_Θ. A heating period of variable length is followed by a brief off period in which the temperature sensitive parameter (TSP) is measured. The transient thermal response is determined by measuring the junction-to-case temperature differences for heating power pulses of different widths; the maximum pulse width used is that which produces steady-state heating in the device under test. An advantage of this technique over the cooling curve method normally used is that the sensitivity of the measurement of the TSP to a change in junction temperature can be increased by increasing the magnitude of the power pulse. This increased sensitivity occurs because one is not limited to the magnitude of the heating power used for steady-state R_Θ measurements when short power pulses are employed.

Further consideration was given to the expectation that the sensitivity to voids of the transient thermal response is greater than that of the steady-state thermal resistance. It can be shown that for most semiconductor devices at least three distinct thermal time constants exist. The shortest of these is associated with the solder used to attach the chip to the case. A somewhat longer time constant is associated with the silicon chip itself, and a still longer time constant, with the case [2].

---

* Transient thermal response is the change in temperature difference (degrees Celsius) between the junction and a reference point which results during a time t (seconds) from the application of a power step of magnitude P (watts).

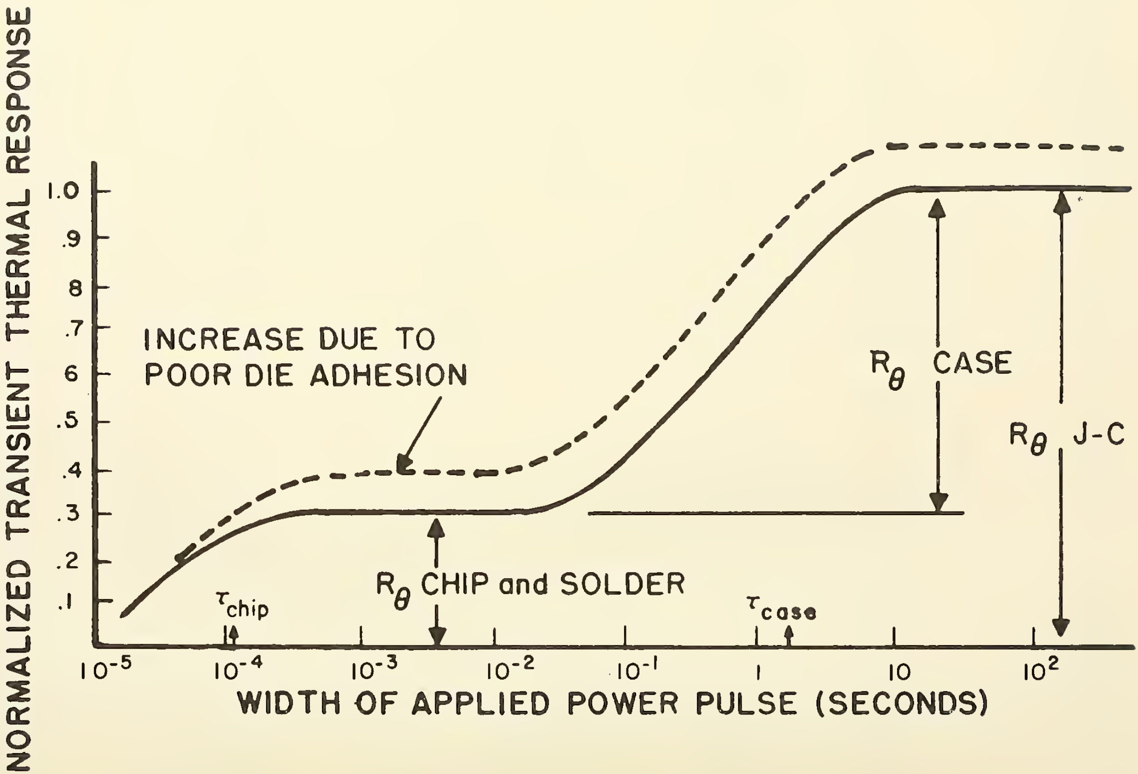

Fig. 9 Transient thermal response normalized to its steady state value as a function of the width of the applied power pulse. The dashed curve represents the increase in thermal response due to poor die adhesion equivalent to a 10 percent increase in junction-to-case thermal resistance (R_ΘJ-C). The width of the applied power pulse is equivalent to the time after initiation of a power step of the same magnitude. Chip and case thermal time constants are also indicated.

Although the solder time constant is usually orders of magnitude less than the chip time constant and cannot be directly observed, the thermal resistance and capacitance of the die-attachment material cause a perturbation of the chip thermal response because the chip precedes the die-attachment material in the thermal path. If the chip time constant is much shorter than the case time constant, a plateau in the transient thermal response curve occurs as shown in Fig. 9. This plateau contains contributions from both the chip and solder thermal resistance. The thermal resistance due to the solder represents a larger fraction of the total in this region than in the steady state case. Hence, measurement of the transient thermal response is more sensitive to poor die adhesion if the width of the applied power pulse is approximately one to five chip time constants in duration. In the example in Fig. 9, a change in the thermal resistance due to poor die adhesion which would result in an increase of 10 percent in the steady-state value would result in over a 30 percent increase of thermal response measured with a power pulse 1-ms wide.
(F. F. Oettinger and R. L. Gladhill)

Procedures for attaching diode chips to headers were established. A modified commercial die bonding machine is now being used in this process. Various methods for incorporating voids into the die bonds in a controlled manner have been proposed. Studies of one method which involves the use of a spherical grinding tool to remove the gold plating from a well-defined area on the header were initiated. (T. F. Leedy)

Plans: The design and fabrication of equipment to be used to measure thermal resistance and transient thermal response of diodes with controlled voids will continue. Investigation of methods for incorporating voids under the diode chip will continue. Processing of diode chips which was delayed because of difficulties with scribing and breaking will be resumed.

3.3 WIRE BOND EVALUATION

Objective: To survey and evaluate methods for characterizing wire bond systems in semiconductor devices and, where necessary, to improve existing methods or develop new methods in order to detect more reliably those bonds which will eventually fail.

Progress: To evaluate the significance of motion of the bonding tool with respect to the work stage on the occasional lift-off or weak bond in a series of otherwise strong bonds, scanning electron microscope photomicrographs have been made of ultrasonic wire bonds formed while the bonding equipment was subjected to intentional motion. Preliminary investigations were carried out on a new bond screening test which consists of applying ultrasonic energy to each individual bond loop. A magnetic detector suitable for tuning ultrasonic wire bonding machines on production lines has

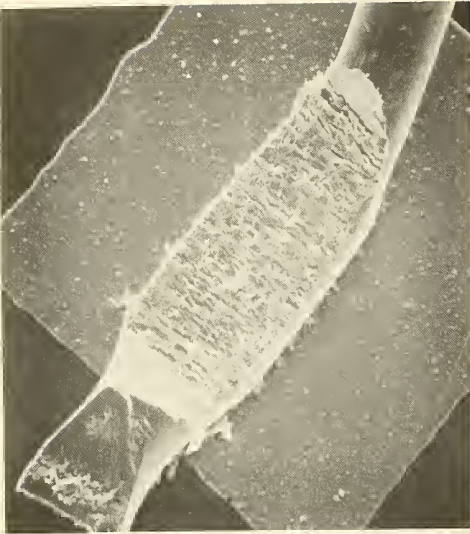

a: Zero motion.

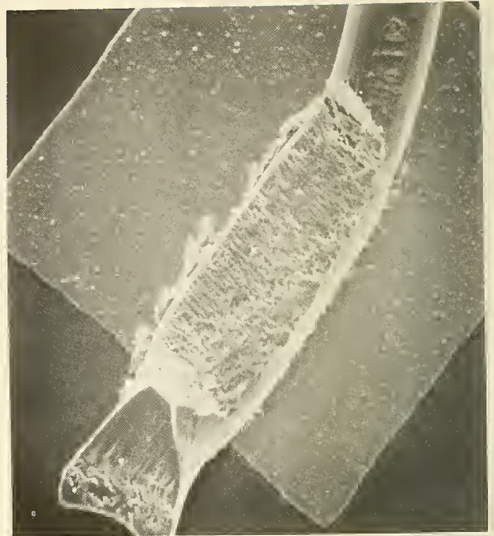

b: 0.0005-in. motion.

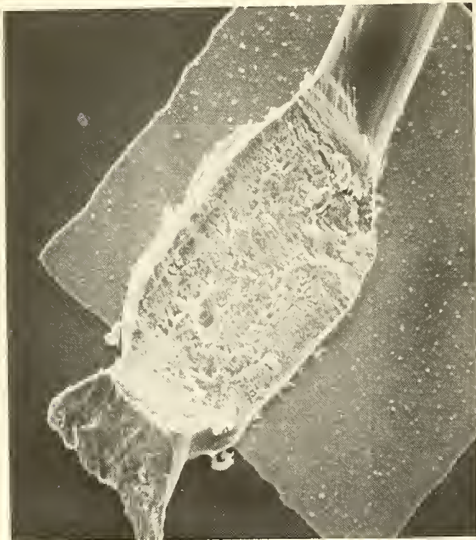

c: 0.0015 to 0.002-in. motion.

Fig. 10 Typical SEM photomicrographs (approximately 500X) of first bonds made with varying amounts of intentionally introduced work-stage motion. Note that there is increased deformation of the wire, unequal extrusion of material from between the wire and bonding pad, and smearing of the tool marks on the top of the deformed wire as the amplitude of the motion increases.

been devised as a simpler, more rugged substitute for the capacitor microphone. A laser interferometer system for measuring absolute displacement of the bonding tool tip has been assembled. The first draft of the section on evaluation methods to be included in the critical review is nearing completion.

Characterization of Ultrasonic Bonding Systems — Capacitor-microphone displacement measurements reported previously revealed a lack of mechanical rigidity in some bonding machines (NBS Tech. Note 527, p. 39). This results in unintentional movement of the bonding tool, held by the transducer, with respect to the transistor or integrated circuit, held by the work stage. Such movement can be transmitted to the machine in a number of ways, including motion of the arm of the bonding operator as it rests on the machine, motion of the work stage as a result of poor mechanical design, or operator movement if the work stage is rotated by hand. In the last case it has been observed that a slight twitch of the hand can result in work stage movement on a typical machine of greater than 0.001 in. With respect to machine instability, the torque of the programming cam motor may produce detrimental vibrations. If any of these occur during the actual bonding period, a lift-off or low pull-strength bond may result.

Experiments were conducted in which work-stage motion was intentionally introduced during the bonding period to characterize the effects of such motion. The motion was introduced by mechanically driving the work stage with an electro-mechanical transducer at various frequencies and displacements. Bonds were observed visually and with the scanning electron microscope. As the degree of motion increased, the bond deformation began to vary widely from bond to bond and an increasingly greater number of lift-off bonds were produced than is normal. With motion of the order of 0.001 in. more than half of the bonds lifted off. Typical bond topographies which resulted from these tests are shown in Fig. 10.

(K. O. Leedy and G. G. Harman)

The use of a capacitor microphone for trouble-shooting and tuning bonding machines has been previously described (NBS Tech. Note 520, pp. 63-66). Efforts have been made to develop a simpler, less expensive, and more rugged system for measuring the vibration amplitude of the bonding tool and for tuning ultrasonic wire bonders on production lines. It was previously noted that magnetic detectors were sensitive to the vibration of bonding tools (NBS Tech. Note 495, p. 25). At that time the magnetic units were being considered for use as in-process bond quality control monitors. However, the physical size of these detectors discouraged an extensive study of their use for this purpose. Interest was revived recently when microphone measurements revealed the importance of properly tuning the ultrasonic system to maximize the bonding tool tip amplitude. Compared with the microphone, the signal from the magnetic detector is relatively insensitive to its distance from the vibration tool. This feature makes it easier to use in reestablishing the tool tip

vibration amplitude after changing tools or in retuning. However, for the same reason, it is less useful than a microphone for investigating the mechanical stability of the bonding machine. The dimensional resolution at the bonding tool of the presently available magnetic detectors is about 0.05 in., which is adequate for tuning pruposes. The magnetic detectors used in this study are approximately one-half inch long are are mounted inside a 10-32 NF screw [1]. This detector system is rugged enough to be used on an assembly line. The detectors are also sensitive to the motion of non-magnetic metal at the vibration frequency of approximately 60 kHz. Thus, it is possible to detect both vibrations along the transducer horn and leakage of ultrasonic energy into the transducer mount. Vibration of the tool tip is observed at distances of about 0.001 in. Signals from the magnetic fields near the magnetostrictive element at the rear of the transducer can be detected when the detector is located up to one-quarter inch from the source. (H. K. Kessler)

A laser interferometer system was constructed to make quantitative measurements of the vibration amplitude of the ultrasonic bonding tool during tuning of the machine and also during actual bonding operation. The principal of the interferometer has been described by Clunie and Rock [2]; specific details were obtained from Martin [3]. The system uses a helium-neon milliwatt laser in which energy is emitted from both ends. Part of the light from the front which is reflected back from the bonding tool modulates the light emitted from the rear of the laser tube. This modulated beam is detected by a light-sensitive silicon diode. The system has produced signals from a vibrating bonding tool which were similar to those shown previously (NBS Tech. Note 520, p. 42). (G. G. Harman)

Capacitor microphone measurements on the bonding tool ultrasonic vibration amplitude and the mechanical stability of a number of bonding machines on a commercial line were made at the request of a sponsor. A summary of these measurements was reported directly to the sponsor.
(H. K. Kessler and G. G. Harman)

An extensive investigation of the effect of bonding machine parameters such as ultrasonic power, pressure, and time, on bond pull strength was begun. The results of pull tests on both the first and second bonds are individually evaluated statistically. Bonding tools with both sharp and rounded heels were used in the tests. The initial results showed that when a 0.0005-in. radius rounded-heel tool was used, the distribution of bond strength with applied ultrasonic power was narrower for the second bond than for the first bond. The opposite case was observed for bonds made with a sharp-heel tool. (K. O. Leedy)

Non-Destructive Screening Test — The use of ultrasonic excitation of completed transistors and integrated circuits in a liquid bath as a failure screen has been reported [4]. A novel method for testing individual bond pair quality which is based on a different form of ultrasonic

excitation was devised and is currently being investigated. This test is performed on an ultrasonic bonding machine by touching the bond loop with the front of the tip of a bonding tool, as shown in Fig. 11, and then applying an ultrasonic pulse to the tool with the power supply control set near its maximum value. The vibration which is induced in the loop causes many bonds to lift off or break at the heel. Presumably, these bonds are weak ones which would eventually fail. In contrast to these, ultrasonic bonds made with 0.001-in. diameter aluminum wire with power, time, and pressure settings adjusted to achieve maximum bond-pull strength yield bonds with pull strengths in excess of 6 grams force even after exposure to such ultrasonic excitation for more than 10 s. In addition to bond quality screening, the method appears to offer a means of assessing damage inflicted on a bond pair by prestressing or other physical means of evaluating bond quality. Although there is qualitative agreement with bond pull data on similar bonds, it should be observed that the method has not been completely evaluated at this time. Optimum values have not yet been established for frequency, ultrasonic power, time of exposure to the ultrasonic vibration, and probe design. As yet there has been no statistical correlation between failure observed by this test and that observed by other tests. (G. G. Harman)

Scanning Electron Microscopy — A special study which was undertaken at the request of a sponsor was completed. The study involved topological examination with the scanning electron microscope of every bond on a number of high-reliability integrated circuits that had passed a variety of the screening tests usually specified for high-reliability devices. Problems such as poor metallization, variable bond deformation, and multiple rebonding were observed. A report consisting of over 90 scanning electron microscope photomicrographs was prepared for the sponsor; it is being modified for issuance as a Technical Note. Another report is being prepared which describes in detail the techniques for examining bond lift-off patterns (NBS Tech. Note 527, pp 42-43) and the results obtained from these studies. (K. O. Leedy)

Bibliography and Critical Review — Detailed analyses of the destructive double-bond pull test and the centrifuge test have been prepared as part of the section on evaluation methods of the critical review. Because of the absence of such information in the literature searched, these analyses, which include the calculation of the relationships between the test stress and the resulting tensile stress along the wire, are summarized here.

The *pull test* is one of the most widely used methods for evaluating the quality of wire bond systems. In its basic form, the test consists of pulling on the wire span between the bond on the terminal and the bond on the die with a hook assembly until rupture of the wire bond system occurs. The pulling force which produces rupture is typically referred to as the bond or pull strength of the system. This test stress is customarially given in units of grams force.

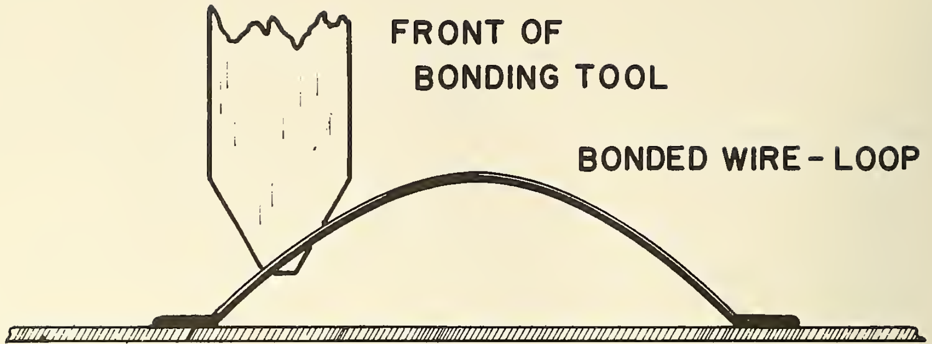

Fig. 11 Placement of bonding tool on bond loop for ultrasonic vibration screening test.

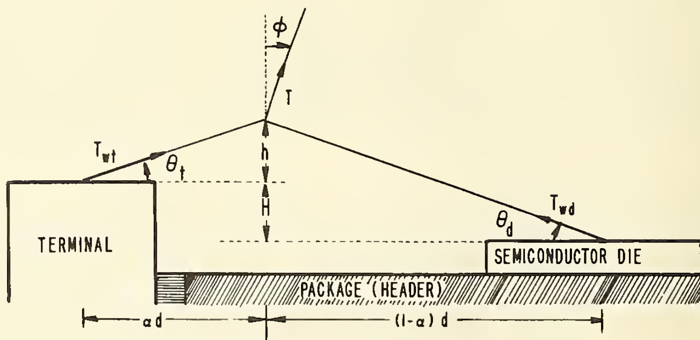

Fig. 12 Geometric parameters for the destructive, double-bond pull test.

The present analysis is intended to provide relationships between the pull strength as described above and the actual force in the wire which results in rupture. As shown in Fig. 12, the direction of the force, T, applied by the hook is inclined an angle ϕ with respect to the normal to the die surface. At the bond on the die the angle between the wire and the die surface is denoted by Θ_d. At the terminal the angle between the wire and the plane of the die surface is denoted by Θ_t. The forces along the wire on the terminal and die sides, T_{wt} and T_{wd}, are related to the force T in the following way:

$$T_{wt} = T \times \frac{\cos(\Theta_d - \phi)}{\sin(\Theta_t + \Theta_d)}, \text{ and}$$

$$T_{wd} = T \times \frac{\cos(\Theta_t + \phi)}{\sin(\Theta_t + \Theta_d)} .$$

The contact angles Θ_t and Θ_d in turn depend on the height, h, of the wire span above the terminal contact surface, the height difference, H, between the plane of the die and the terminal contact surface, and the horizontal distances, αd and $(1 - \alpha)d$, from the bonds to the point at which the wire span is contacted by the hook.

If $2\Theta_d + \Theta_t - \phi < 90$ deg the wire tensile force on the terminal side of the hook will be greater than the applied force at the hook. Similarly, if $2\Theta_t + \Theta_d + \phi < 90$ deg the wire tensile force on the die side of the hook will be greater than the applied force at the hook. For various fixed ratios of Θ_d to Θ_t and for $\phi = 0$ the ratio T_{wt}/T as a function of Θ_t is shown in Fig. 13. These curves are also valid if the subscripts d and t are everywhere interchanged. They indicate how dramatically the tensile force in the wire may differ from the test stress applied at the hook. They also show that wire bond systems with different contact angles may have entirely different tensile forces for the same applied pulling force.

The dependence of the ratio T_{wt}/T on the value of ϕ is also indicated in Fig. 13. The effect of varying ϕ by ±5 deg is shown by the horizontal bars on either side of the curves for $\Theta_d/\Theta_t = \frac{1}{2}$ and 2. Positive values of ϕ result in greater tensile force along the wire. The dependence of T_{wt} on ϕ increases with the ratio $(\Theta_d - \phi)/(\Theta_t + \Theta_d)$. The symmetry between T_{wt} and T_{wd} is maintained if the sign of ϕ is reversed at the same time the subscripts d and t are interchanged.

The ratio of the tensile force on the wire at the terminal to the tensile force in the wire at the die is given by:

$$\frac{T_{wt}}{T_{wd}} = \frac{\cos(\Theta_d - \phi)}{\cos(\Theta_t + \phi)} .$$

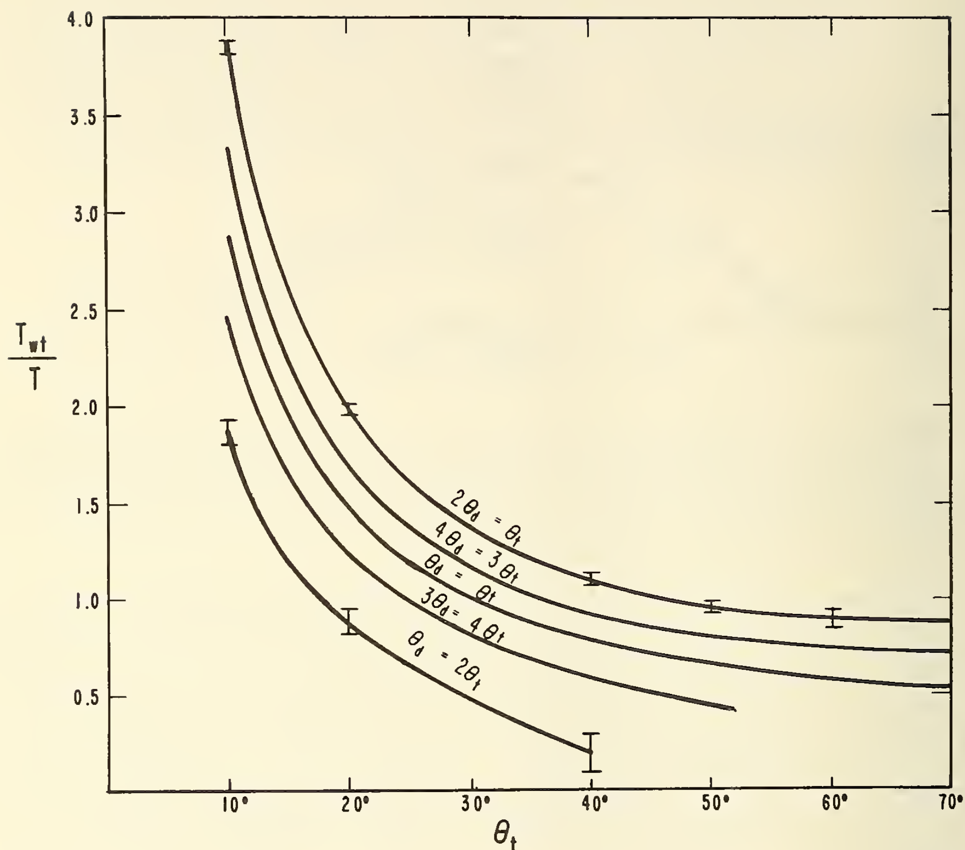

Fig. 13 Dependence of T_{wt}/T and Θ_t for various ratios Θ_d to Θ_t. The curves are for the case $\phi = 0$. Horizontal bars above and below the curves for $\Theta_d = \frac{1}{2}\Theta_t$ and $\Theta_d = 2\Theta_t$ show the effect of changing ϕ to plus and minus 5 deg, respectively. To obtain the dependence of T_{wd}/T, interchange everywhere the subscripts d and t and change the sign of ϕ.

Because H is usually positive, Θ_t is usually less than Θ_d. In most cases ϕ is small; consequently it is quite likely that T_{wt} is less than T_{wd}. For this case, changes in ϕ have a greater effect on T_{wt} than on T_{wd}. This is of particular importance in studying ultrasonic wire bond systems in which the first bond has been made on the terminal surface because the first bond is frequently the weaker bond. The measured tensile force at failure in such systems may be quite sensitive to the value of ϕ.

Although the geometrical dependence is more easily visualized in terms of the angles Θ_d and Θ_t, these angles are difficult to measure. Because they depend in known ways on the parameters h, H, d, and α, it is appropriate to consider the sensitivity of the test to these parameters. If the parameters are determined for each case, it is possible to determine the extent to which the distribution of pull strengths observed is actually due to variations in the quality of the wire bond system being tested. Such an analysis can also assist in determining which parameters are the most important to control.

The *centrifuge test* subjects a device to a constant acceleration in order to determine the ability of component parts of the device to sustain the force imposed. The test is widely used to cull out defective bond systems fabricated with gold wire. The lower density of aluminum makes this test less useful for systems fabricated with aluminum wire.

In the test the device is oriented so that the force is directed normal to and away from the contact surfaces. If it is assumed that the wire between the bonds describes a catenary curve, the tensile stresses, T_{wt} and T_{wd}, in the wire adjacent to the terminal and die bond respectively, can be calculated in units of grams force:

$$T_{wt} = \rho \, \pi r^2 \, G \, (a + h), \text{ and}$$

$$T_{wd} = \rho \, \pi r^2 \, G \, (a + h + H),$$

where $a \simeq d^2/\{4h[1 + \sqrt{1+(H/h)}\,] + 2H\}$, for $d/(h + H) \geq 2$,
ρ = density of the wire, g/cm^3,
r = radius of the wire, cm,
h = vertical distance between the terminal contact surface and the apex of the wire loop, cm,
H = vertical distance between the die and terminal contact surfaces, cm
d = horizontal distance between bonds, cm, and
G = centrifugal acceleration, gravity units.

The approximation for a is in error by less than 10 percent for $d/(h + H) = 2$. For the unusual case when the wire bond system is such that $d/(h + H)$ is significantly less than 2 it is necessary to solve the exact expression, $h + H + a = a \cosh(D/2a)$, where D/2 is the lateral distance between the die contact and the apex of the wire.

These relationships allow the evaluation of the usefulness of a specific acceleration level in the screening of particular systems. As an example, consider a simple system where the bonds are made in the same plane, the bond separation is 2 mm, and the height of the loop during the test is 0.3 mm. For an acceleration of 30,000 g's, the stress in the wire adjacent to the bond is about 0.58 grams force (5.7 mN) for a 25-μm diameter gold wire. A bond system which would rupture when this tensile stress is reached would also rupture with a measured pull strength of only about 0.39 grams force (3.8 mN). (H. A. Schafft and E. C. Cohen)

Plans: The laser interferometer system will be completed and used for an absolute measurement of bonding tool vibration amplitude. Evaluation of ultrasonic bonding machines will continue; further assistance will be given to sponsors in connection with problems encountered on production lines. Statistical studies for optimizing bonding parameters will be continued. Experiments with the purpose of evaluating the importance of bonding machine parameters with respect to bond pull strength will be continued. Experimental and statistical analysis of significant factors in the bond pull test will begin when suitably reproducible bonds can be made for the test structure. Scanning electron microscope studies of bond lift-off patterns will be continued in order to develop a fuller understanding of the mechanism of bond formation. Additional scanning electron microscope studies will be used in the evaluation of different tool designs. Work on modification of the bond puller and wire tester will continue. Work on the critical review and on compilation of the bibliography will continue.

3.4 PROCESSING FACILITY

Objective: To establish a microelectronics fabrication laboratory consisting of the facilities and procedures necessary for the production of specialized silicon devices for use in research on measurement methods.

Progress: Procedures for producing a bipolar test slice have been developed. The slice contains arrays of a structure, shown in Fig. 14, composed of three diffused resistors, a diode, and a transistor. The planar *n-p-n* transistors are intended to have a common-emitter current gain (h_{FE}) of 30 to 50 so that they are compatible with TTL or RTL circuits.

As a result of excessively wide base width the first set of devices fabricated had very low gains ($h_{FE} \approx 1$). By adjusting the emitter drive-in time, h_{FE} was improved to about 30. In some cases when the base width was exceedingly small, the devices were punch-through limited, and h_{FE} as high as 150 was noted. Values for the base-collector junction breakdown voltage and leakage current could be obtained from the diodes. A rough

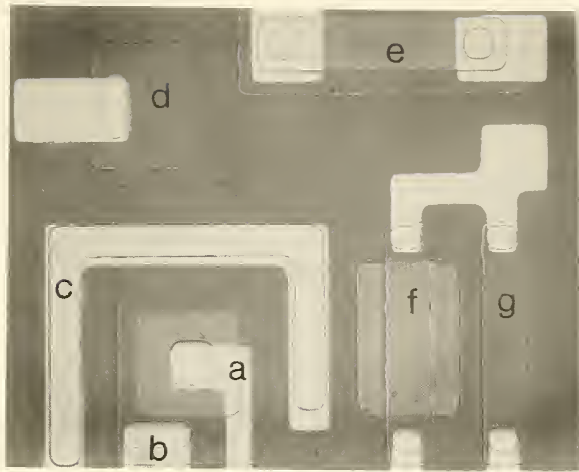

Fig. 14 Photomicrograph of bipolar test chip. The parts of the test chip are: a, transistor emitter; b, transistor base; c, transistor collector; d, diode; e, emitter resistor in base diffusion; f, pinched base resistor; and g, base resistor. (Magnification: 65X).

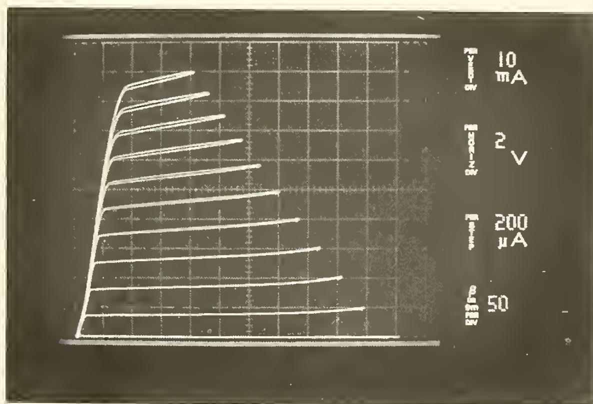

Fig. 15 Common emitter characteristic of *n-p-n* transistor in bipolar test chip.

idea of the sheet resistance of both the emitter and base diffusions could be obtained from measurements on the diffused resistors.

A typical set of characteristic curves for the transistor operating in a common-emitter configuration is shown in Fig. 15. Collector-emitter breakdown voltages of about 25 V were observed on most of the slices that were produced by the process which yielded the desired value for h_{FE}.

A method, adapted from published techniques [1], was developed to chemically-mechanically polish silicon wafers. Wafers finished by this technique were characterized by their flatness (±2 fringes across a 1.5-in. diameter wafer) and their freedom from surface damage as viewed with a scanning electron microscope.

A procedure for using negative-working photoresists was developed. By adjusting the viscosity and film thickness, the process was made as compatible as possible with the presently used positive-working photoresist process. Use of negative-working photoresist has the advantage of freedom from some types of contamination encountered when using positive-working photoresist. (T. F. Leedy and J. Krawczyk)

Work was completed on the platinum-bonded, silicon-sandwich temperature sensor for use in controlling the substrate temperature during evaporation (NBS Tech. Note 495, p. 21). The cracking problem encountered in the early stages of construction was solved by the use of a thinner platinum solder-foil and by firing the bond in a dry hydrogen atmosphere. Construction details are given in the exploded view shown in Fig. 16. When assembled, the sensor has nearly the same thermal characteristics as a silicon wafer. One of the two thermocouples in the sensor drives a null-balance controller which regulates the radiant heating system (NBS Tech. Note 488, p. 19) in the evaporator. The substrate temperature is measured directly with the second thermocouple and a millivolt potentiometer. The sensor is usable up to a temperature of 830°C before the platinum-silicon bond fails.

To determine the temperature control sensitivity of the system a series of experiments was conducted near the gold-silicon eutectic temperature (370°C). Gold was deposited at various preset temperatures both above and below the eutectic temperature on exposed silicon surfaces which were placed in a quartz mask together with the temperature sensor under the radiant lamps. Freshly cleaned silicon wafers were used for each evaporation. Following evaporation the silicon surfaces were examined for eutectic formation. From direct thermocouple measurement and microscopic examination of the coated wafers, it is estimated that the surface temperature was controlled within ±2.0°C at 370°C. Although there was noticeable heating of the substrates by the evaporation sources, the control system was apparently able to compensate rapidly enough. (W. K. Croll)

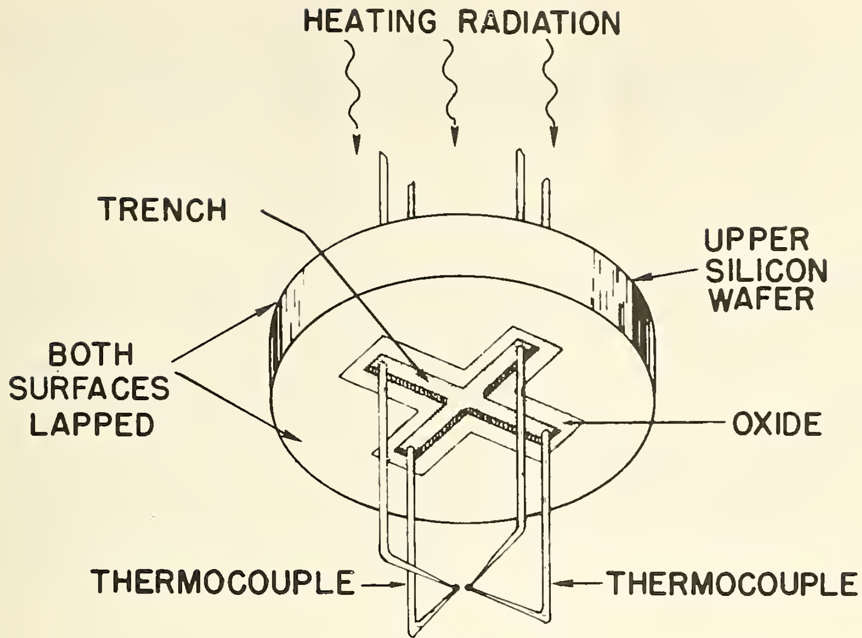

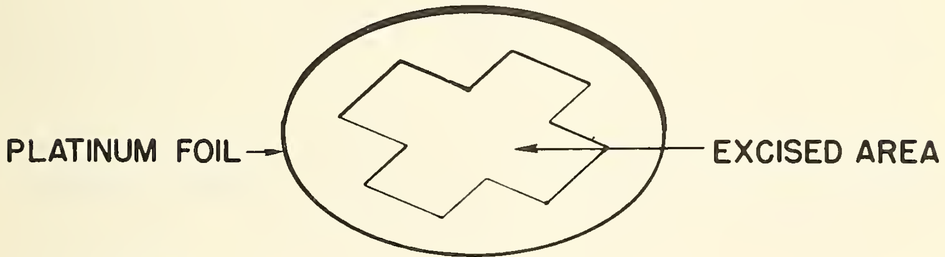

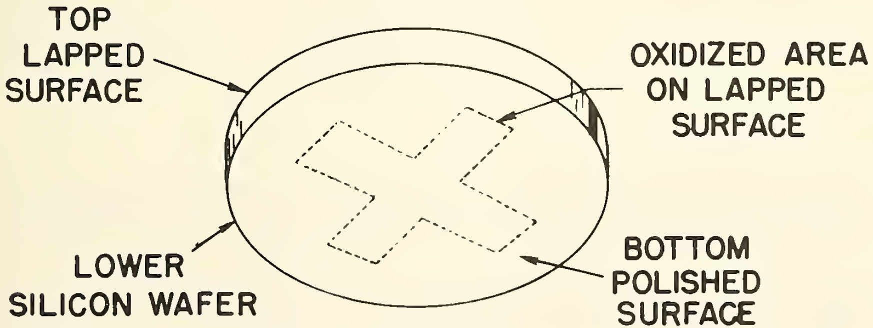

Fig. 16 Detail of platinum-bonded, silicon-sandwich temperature sensor.

Plans: Fixtures which will allow thicker aluminum depositions to be made on monolithic circuits will be designed and built. The new apparatus is also expected to provide more uniform aluminization over oxide steps. Procedures for scribing and breaking wafers will be investigated. Work will begin on fabrication of metal-oxide-semiconductor devices.

3.5 NASA MEASUREMENT METHODS

Objective: To review existing semiconductor test method standards for material and process control measurements and to prepare interim test methods in a standard format as may be appropriate.

Progress: NASA test methods [1] were reviewed with emphasis on comparison of the precision needed to meet the requirements for microcircuit line certification [2] with the precision to be expected from these test methods. Preparation of an extensive table that lists the various test methods, the reference in the line certification document, equivalent ASTM tests where these are available, and the precision requirements and capabilities is nearly complete. In addition tests which are necessary to meet the requirements of NASA line certification but which are not included in the NASA test standards [1] were also identified.

Additional assistance was given ASTM Committee F-1 in the development of standard procedures for leak testing hermetically sealed devices. The procedure for determining the hermeticity of electron devices by means of the bubble test was extensively revised. (W. M. Bullis)

Plans: Work on the table of NASA methods will be completed. It will be revised if necessary to reflect any changes which were made between NASA-STD-XX-6 and the document [3] cited in MIL-M-38510, General Specification for Microcircuits. Areas in need of additional work in order to obtain or confirm the required precision will be identified.

3.6 REFERENCES

3.2 Die Attachment Evaluation

1. R. A. Lockett, H. A. Bell, and R. Priston, "Thermal Resistance of Low Power Semiconductor Devices under Pulse Conditions," *Mullard Tech. Comm.* 76, 146-161 (1965).

2. *RCA Power Circuits, DC to Microwave,* SP-51, RCA Electronic Components, Harrison, N. J. 07029, 1969, p. 95.

3.3 Wire Bond Evaluation

1. One such detector is available from Electro Products Laboratory, Chicago, Illinois. This equipment is identified in this paper in order to adequately specify the experimental procedure. In no case does such identification imply recommendation or endorsement by the National Bureau of Standards, nor does it imply that the equipment identified is necessarily the best available for the purpose.

2. D. M. Clunie and N. H. Rock, Jr., "The Laser Feedback Interferometer," *J. Sci. Instrum.* 41, 489-492 (1964).

3. B. D. Martin, presented at New York State Technical Services Symposium on Lasers and Their Application in Local Industries, Binghampton, N. Y., April 14, 1969.

4. G. C. Knollman, A. S. Hamamoto, and J. L. S. Bellin, "Reports on Ultrasonic Screening of Transistors and Integrated Circuits," LMSC B-62-29-8, Lockheed Palo-Alto Research Laboratory, Palo Alto, California 94304 (June, 1969).

3.4 Processing Facility

1. L. H. Blake and E. Mendel, "Chemical-Mechanical Polishing of Silicon," *Solid State Tech.* 13, No. 1, 42-46 (1970).

3.5 NASA Measurement Methods

1. "Test Standards for Microcircuits," Draft of NASA-STD-XX-3 , October 1, 1969.

2. "Microcircuit Line Certification," Draft of NASA-STD-XX-6, December 1968.

3. "Line Certification Requirements for Microcircuits," NHB 5300.4 (3C). Available from Superintendent of Documents, U. S. Government Printing Office, Washington, D. C. 20402.

4. METHODS OF MEASUREMENT FOR SEMICONDUCTOR DEVICES

4.1 THERMAL PROPERTIES OF DEVICES

Objective: To evaluate and, if necessary, improve electrical measurement techniques for determining the thermal characteristics of semiconductor devices.

Progress: The literature search of methods to measure thermal resistance and transient thermal response of semiconductor devices was continued. Because of difficulties in evaluating some of the significant literature, completion of the first draft of the section of the review paper on the measurement of steady-state thermal resistance was delayed. In preparation for the compilation of a bibliography, keywords were assigned to some of the relevant articles on thermal measurements of semiconductor devices. (M. Sigman and F. F. Oettinger)

Analysis of preliminary data taken with the thermal resistance test circuit (NBS Tech. Note 527, pp. 48-50) indicated that non-thermal effects prevented correlation of measurements made under calibration and power-test conditions. Under the low-current, high-voltage operating conditions which are of interest because of the hot-spot hysteresis effect previously observed (NBS Tech. Note 520, pp. 49-52), the base current was chosen to be as small as possible consistent with a linear voltage-temperature characteristic during the interval in which the base-emitter voltage, V_{BE}, was measured. This required a high-impedance (100 kΩ) base-current supply. Since the capacitance associated with the device under test had to discharge through the high-impedance base circuit, this circuit does not permit the fast switching required of both the emitter-base and collector-base junctions. To allow fast switching, low-impedance paths had to be provided for discharge of the junction and distributed capacitances.

Even though the collector of the device under test was open during the measurement of the temperature sensitive parameter, V_{BE}, this does not ensure that V_{BE} was always being measured under the same conditions. It has been observed that the value of V_{BE} depended on the value of the collector-emitter voltage, V_{CE}, during critical periods in the sequence of measuring thermal resistance as illustrated in the small-signal, reverse-voltage transfer ratio curves shown in Fig. 17. For low values of V_{CE}, a small change in V_{CE} causes a significant change in V_{BE}. For example, at a case temperature of 100°C and base current of 0.8 mA, an increase of V_{CE} from 0.0 to 0.2 V causes a change in V_{BE} of 120 mV or an apparent change in temperature of approximately 60°C. Thus, if a switching transistor is used in series with the device under test to open the collector during the measurement of thermal resistance. it may also have to be used when calibrating V_{BE} against temperature. It was found that

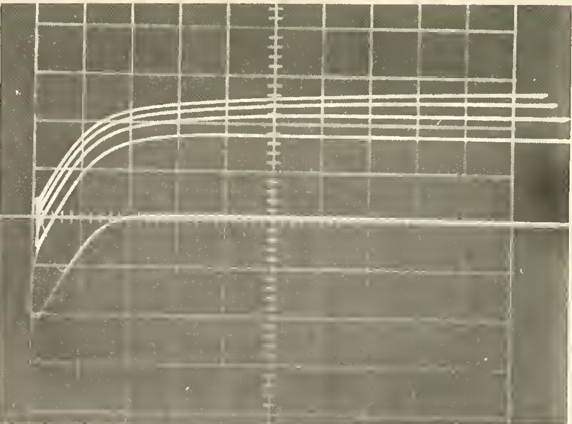

a: Case temperature, 25°C.

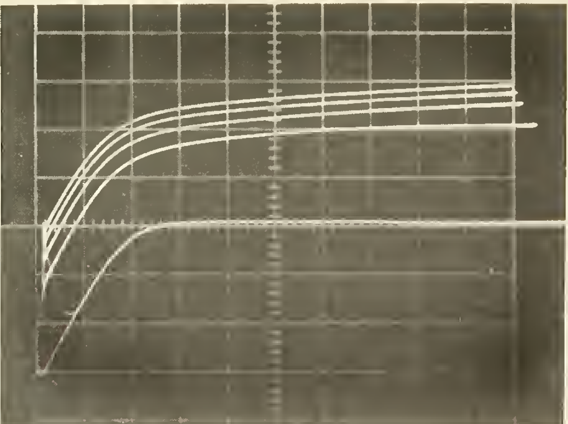

b: Case temperature, 100°C.

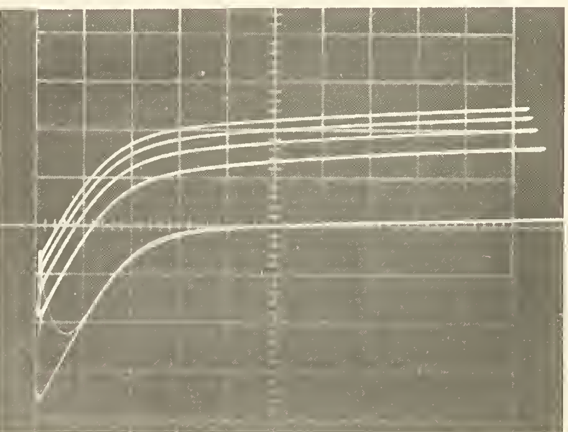

c: Case temperature, 150°C.

Vertical Scale: Base-emitter voltage (0.05 V/div.).
Horizontal Scale: Collector-emitter voltage (0.1 V/div.).

Fig. 17 Small-signal, reverse-voltage, transfer ratio characteristics for a medium power, triple-diffused, *n-p-n* silicon transistor. The base current is stepped from 0 to 0.8 mA in 0.2 mA steps.

under some conditions opening the collector with a series switching transistor does not guarantee that the collector voltage has stabilized by the time that the temperature sensitive parameter is measured. Even though the switching time of the series switching transistor is small compared with the measurement delay time, the collector-emitter voltage may still be changing. Under these conditions it may be necessary to use a voltage clamp to force the collector-emitter voltage to the desired value during the measurement interval.

When the thermal resistance is measured under conditions of high collector voltage and low collector current (I_C = 100 mA) the common emitter current gain, h_{FE}, is often greater than 100. The measuring current used during the V_{BE} measurement (I_B = 650 μA) is then so high that the servo-amplifier is unable to maintain continuous control of the collector current.

To isolate and solve these problems, a cascade monostable multivibrator was designed,† built, and added to the thermal resistance test set. The multivibrator delays the switching of the base current for about 5 μs in order to allow the collector switching transistor to turn off. The multivibrator also switches the base heating current on again after approximately 15 μs. This switching sequence permits a higher V_{BE} measuring current to be used so that a lower impedance base current supply can be employed.

A further advantage of the modified circuit is derived by driving two common-emitter amplifiers from the two outputs of the multivibrator and using separate diodes as switches in the two base current supplies. This modification permits switching from the servo-controlled, heating-current supply to the constant, measuring-current supply and prevents the unstable condition that previously occurred whenever the total base current required to maintain a constant collector current was less than the measuring base current. With logic provided by the multivibrator it is possible to clamp the collector of the device under test to a predetermined low voltage during the measuring interval. Use of this same clamping voltage when calibrating the temperature sensitive parameter to ensure calibration under the same conditions as measurement is being investigated.

Work was also begun on a new heat sink which employs a beryllium oxide insulator between the temperature-controlled portion of the heat sink and the copper washer on which the device under test is seated. Use of beryllium oxide as the electrical insulator permits better thermal exchange between the device under test and the heat sink than the use of

---

† This circuit was designed by D. Brenner, Measurement Engineering Division.

most other insulating materials. In accord with draft recommendations of IEC TC-47 and JEDEC Committee JS-6, the thermocouple, which is used to monitor the case temperature of the device under test, is embedded in the copper washer.

The study to determine the merits of fully automating the thermal resistance measuring system and the study to compare V_{BE} and V_{CB} as temperature sensitive parameters were not undertaken due to a shift in priorities. These studies may be taken up again at a future time.
(S. Rubin, R. L. Gladhill, and F. F. Oettinger)

Increased recognition of the thermal measurement problem in both discrete devices and integrated circuits has led to greater activity in several committees concerned with semiconductor device characterization. Project personnel are participating in the activities of the following committees:

JEDEC Committee JS-1 on Rectifier Diodes — This committee is planning to conduct a round robin on a thermal resistance test method similar to that now being studied by JEDEC Committee JS-14 on Thyristors.

JEDEC Committee JS-2 on Signal Diodes — This committee has instituted a task group to study the need for a preferred test method for measuring thermal resistance of signal diodes. A round robin of the selected test method is also being considered.

JEDEC Committee JS-14 on Thyristors — This committee is involved in a round-robin program to test a referee method for measuring thermal resistance of high-power thyristors.

EIA Committee MED-41 on Physical Characterization Requirements — A task group of this committee is defining parameters and test methods for characterizing the thermal properties of microelectronic devices.

IEC Technical Committee 47, Semiconductor Devices and Integrated Circuits — A secretariat document dealing with nomenclature, definitions, and letter symbols for thermal characteristics of semiconductor devices is being circulated to the U. S. National Committee of the IEC for comment.
(F. F. Oettinger)

Plans: The literature search and work on the bibliography will continue. The first draft of the review paper on steady-state thermal resistance measurements will be completed.

After completion and checking of the modifications to the semiautomated measuring system, measurements will be continued both of thermal resistance and h_{FE} as a function of collector-emitter voltage on power transistors. Fabrication of the new temperature-controlled heat sink will be completed.

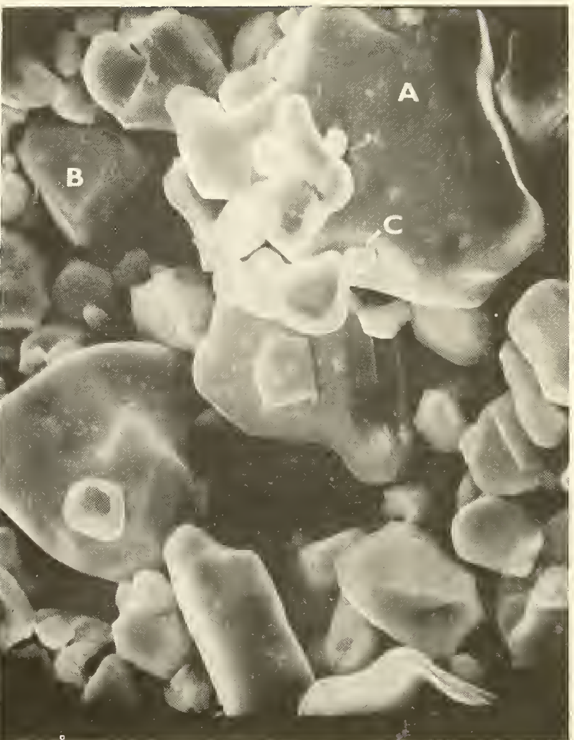

a: Extremes of particle size. The longest dimension of particle A is 25-μm; particle B is 9-μm on a side; particle C is about 2.5-μm long.

b: This cluster of small particles appeared to be a single large particle at lower magnification. The long dimension of particle A is 12-μm; particle B is 9-μm on a side.

Fig. 18 SEM photomicrographs (2000X) of thermographic phosphor particles of nominal 9-μm size.

4.2 THERMOGRAPHIC MEASUREMENTS

Objective: To evaluate the utility of thermographic techniques for detection of hot spots and measurement of temperature distribution in semiconductor devices.

Progress: Work has been devoted principally to temperature calibration of the thermographic phosphors and examination of their particle size and coating uniformity. Experiments have been carried out to determine the most sensitive ranges of the several phosphors for different levels of ultraviolet illumination. When completed, a chart of these data can be used to select the optimum combination of phosphor type and ultraviolet illumination for maximum sensitivity to temperature changes for any 50-deg interval within the temperature range between 25 and 400°C.

Use of the scanning electron microscope to examine a silicon wafer coated with thermographic phosphor revealed the coating to be fairly uniform with particle sizes varying from about 2.5 to 25 μm. The average particle size appears to be about 9 μm as stated by the manufacturer of the phosphors. The variation in particle size is illustrated in Fig. 18. Each picture is an enlargement of an area approximately 45 μm by 55 μm.

For the study of spatial resolution of the phosphors a test fixture has been fabricated which can be used with both the photometric and infrared microscopes.

(G. J. Rogers, F. F. Oettinger, and L. R. Williams, Jr.)

Plans: The temperature calibration of the phosphors will be completed. Studies of spatial resolution using both the phosphors and the infrared microscope will begin. After the electrical characterization of the thermal properties of transistors is complete, the surface temperature characteristics of these transistors will be studied with the phosphors.

4.3 MICROWAVE DEVICE MEASUREMENTS

Objective: To study the problems and uncertainties associated with the measurement of microwave device properties and to improve the methods for measuring the characteristics of these devices.

Background: During World War II a variety of measurement methods for mixer and video detector diodes were devised at the MIT Radiation Laboratory [1]. Many of these methods are still in common use. In the years immediately following the war, two military laboratories were responsible for tuning standard mixer-diode holders and for calibrating sets of standard mixer diodes. The standard diodes were used by diode manufacturers to calibrate local oscillators and modulation-method conversion loss measurement equipment. This activity was ended at both laboratories more than ten years ago.

Following the loss of the government calibration system, microwave diode manufacturers relied largely on their own internal standards. They attempted to maintain product uniformity and consistency largely from relative, rather than absolute, measurements. The few manufacturers of similar devices checked their measurements against each other on an informal basis. The lack of formal calibration and the inadequacies in existing test methods have led to a number of severe problems.

Of particular concern to diode manufacturers are the provisions in MIL-STD-750, Test Methods for Semiconductor Devices, which require traceability of the measurements to NBS and establishment of a guard band to account for measurement uncertainty. The standard requires that manufacturers determine their measurement uncertainties and that they stay within specification limits by at least the amount of these uncertainties. Because of the insistance of some manufacturers that it is impossible for them to comply with this provision, it has not been enforced. However, these requirements were restated in the individual specification sheets for the new low-noise military grades of 1N21 and 1N23 mixer diodes, the 1N21WG and 1N23WG. The noise figure limits for these new grades were set to such a low value that the manufacturers claimed that the yield would be unacceptably low. On the other hand, if the noise figure limits were increased to make room for the guard band, the limits would be identical with those for non-premium grades.

In order to resolve this problem, the 1N21WG and 1N23WG specifications were revised to permit the use of a round robin to adjust differences in systematic error between manufacturers and to set guard bands to compensate only for random errors. Although the initial formal round robin data from the three manufacturers of the low-noise diode types were quite similar, the noise figure quoted is still not referenced to a fundamental standard.

Progress: Representatives of NBS, the military services (U. S. Navy Electronic Systems Command and Defense Electronics Supply Center), and industry (JEDEC Committee JS-3 on UHF and Microwave Diodes) have met frequently during the last 18 months to establish a program to assist in solutions of these and some related problems. As a result of these meetings the requirements of government and industry in this area have been defined sufficiently and initial resources obtained to begin an active program.

The principal needs are standards documents with precise definitions and standard measurement procedures published by the appropriate organizations. The role of NBS in this work is the study of new or improved measurement methods. For any method, this study includes detailed analysis of the test conditions, measurement equipment, and test fixtures, identification of the required calibration and transfer standards, and establishment of the precision of the measurement.

The parameters which require study are numerous. They range from the properties of classic radar detection crystals to those of new solid state sources and microstrip devices. Initial work is being conducted on mixer diodes and microwave transistors. Plans have been made for work to be conducted both within the Joint Program and with the assistance of the Radio Standards Engineering Division at the NBS Boulder Laboratories. Four areas have been selected for initial work on mixer diodes: noise, mixer diode conversion loss, mixer diode r-f and i-f impedance, and mixer diode burnout. In addition, requirements for microwave transistor measurements are being surveyed.

Mixer Diodes — First priority is being given to the measurement of mixer diode noise, including all of those parameters that contribute to the overall receiver noise performance: mixer output noise, conversion loss, r-f and i-f immittances, i-f amplifier noise and input immittances, and r-f source immittance at all significant frequencies. In order to study the interaction between these parameters and to compare the various methods of measuring each of them, a single X-band system is being assembled in which all of the parameters can be measured in rapid sequence and the same parameter can be measured by different methods. The nearly simultaneous determination of all parameters in the same set-up is expected to reduce errors which may arise from a variety of sources.

Mixer diode characterization is required at a minimum of 15 discrete frequencies between 1 and 95 GHz. Measurements over this entire range would require a large number of expensive measurement systems. Because the most urgent measurement problems can be identified from measurements at a single X-band local-oscillator frequency, 9.375 GHz, initial work on 1N23 crystals is being undertaken at this frequency. At the same time consideration is being given to broadband coaxial techniques which are expected to permit measurements to be made more economically the long run. Equipment is also being assembled to compare the various techniques for measuring diode impedance and to obtain data from which the errors inherent in the measurement methods can be analyzed.

In addition to the experimental work, the various measurement techniques and definitions for mixer diode noise are being reviewed. A survey is being conducted to determine the problems encountered in the various techniques now being used to measure conversion loss.

In the area of standard measurement methods for mixer diode parameters, some methods are listed in MIL-STD-750, Test Methods for Semiconductor Devices, and in an IEC TC-47 Draft Document, but these are too brief and imprecise to assure the desired degree of reproducibility. The IEEE-GED Standards Committee for Electron Devices has set up a task group, Solid State Microwave Devices II, to deal with some aspects of mixer and video detector diodes, with J. M. Kenney as chairman. In addition, liaison is maintained with JEDEC Committee JS-3 on UHF and Microwave Diodes which has been concerned with this problem for some time.

Transistors — A survey to determine the measurement requirements and status for microwave transistors has been undertaken. One of the primary problems is to choose between specification of voltage-current properties as measured on a sampling oscilloscope, impedance properties as measured on a bridge and slotted line, or scattering parameters as measured on reflectometers and network analyzers. Another problem is the lack of standards and calibration services for calibrating transistor test mounts and fixtures.

An analysis of scattering parameter measurement problems has been undertaken in cooperation with the S-parameter task group of JEDEC Committee JS-9 on Low Power Transistors. (J. M. Kenney and R. C. Powell)

Plans: Study of mixer diode noise will continue, but the time required for selection and delivery of apparatus will probably preclude much experimental work during the next quarter. The survey of techniques being used for measuring noise figure, conversion loss, impedance, and other parameters for mixer diodes will continue. Assembly of apparatus to measure the power handling capability of mixer diodes (burn-out rating) and analysis of methods for measuring burn-out will begin. An investigation of the feasibility of employing coaxial microwave apparatus will begin. The survey of transistor measurement requirements will continue.

4.4 SILICON NUCLEAR RADIATION DETECTORS†

Objective: To conduct a program of research, development, and device evaluation in the field of silicon nuclear radiation detectors with emphasis on the improvement of detector technology, and to provide consultation and specialized device fabrication services to the sponsor.

Progress: The space simulation chamber for life testing of detectors was modified to accommodate up to 21 silicon detectors. Extensive preflight testing of detectors for the sponsor continued. Design work on the automated testing system was completed. Radiation damage effects of 200- and 400-keV electrons in surface-barrier detectors were investigated.

Testing and Evaluation — To evaluate detectors for the forthcoming Pioneer F spacecraft experiment the space-simulation test chamber was modified to increase its capacity from 8 to 21. Fourteen totally-depleted detectors for the package plus seven spare units can be tested at one time. Because of severe space limitations within the vacuum chamber, a special

---

† Supported by Goddard Space Flight Center, National Aeronautics and Space Administration. (NBS Project 4254429) Irradiations were carried out at Goddard Space Flight Center.

baseplate mounted above the original baseplate was designed on which the detectors lie flat in two concentric rings. Liquid is circulated through the lower baseplate to provide thermal control. Space is provided for the irradiation of both front and rear detector surfaces with alpha particles to monitor detector counting performance. Provisions are made for applying independent bias voltage to each detector. Problems encountered in the adaptation of the chamber for detector life-testing have included space limitations in the chamber, high-vacuum requirements, maintenance of low stray capacitance on the signal leads and thermal stability in the temperature range of -40 to +50°C.

Acceptance and pre-flight testing of surface-barrier detectors for the IMP-I satellite experiment have continued. The circuit design for the automated system for monitoring reverse leakage current, noise, and temperature of large numbers of detectors stored at room temperature has been completed. The system is being wired and assembled by the sponsor.
(B. H. Audet and D. M. Skopik)

The evaluation of silicon-avalanche detectors for counting low-energy electrons has continued with additional testing of detectors which operate in the avalanche mode at about 200 V. The counting performance of these detectors was comparable to that of the 2000-V avalanche detectors reported previously (NBS Tech. Note 520, p. 56). The stability and noise characteristics were better for the low-voltage detectors. As with the high-voltage detectors, the low-voltage devices also showed a relatively low detection efficiency for electrons with energies below 10 keV.
(Y. M. Liu)

Radiation Damage — The gold front contact of a 100-μm thick, totally-depleted, surface-barrier detector at room temperature was irradiated with 200-keV electrons. No significant effects for fluences of up to 10^{16} cm^{-2} were noted. Detector leakage current, capacitance, and full width at half maximum increased slightly with fluence in this range. Since the threshold energy for an electron to displace a silicon atom is approximately 250 keV, very little damage to the bulk silicon was expected. It appears that these relatively low-energy electrons did not produce significant damage effects at the sensitive surfaces of the detector.

Two totally-depleted, 1000-μm thick, surface-barrier detectors were irradiated with 400-keV electrons. Electrons were incident on the front gold contact of one detector and on the rear aluminum contact of the other. Detector leakage current, noise, and full width at half maximum increased with fluence. The detector capacitance at reverse bias voltage below the normal operating point of 150 V decreased with fluence, whereas at the full operating voltage the capacitance increased with fluence. When the detector counting performance was evaluated with Am^{241} alpha particles incident on the irradiated contact, double peaks in the energy

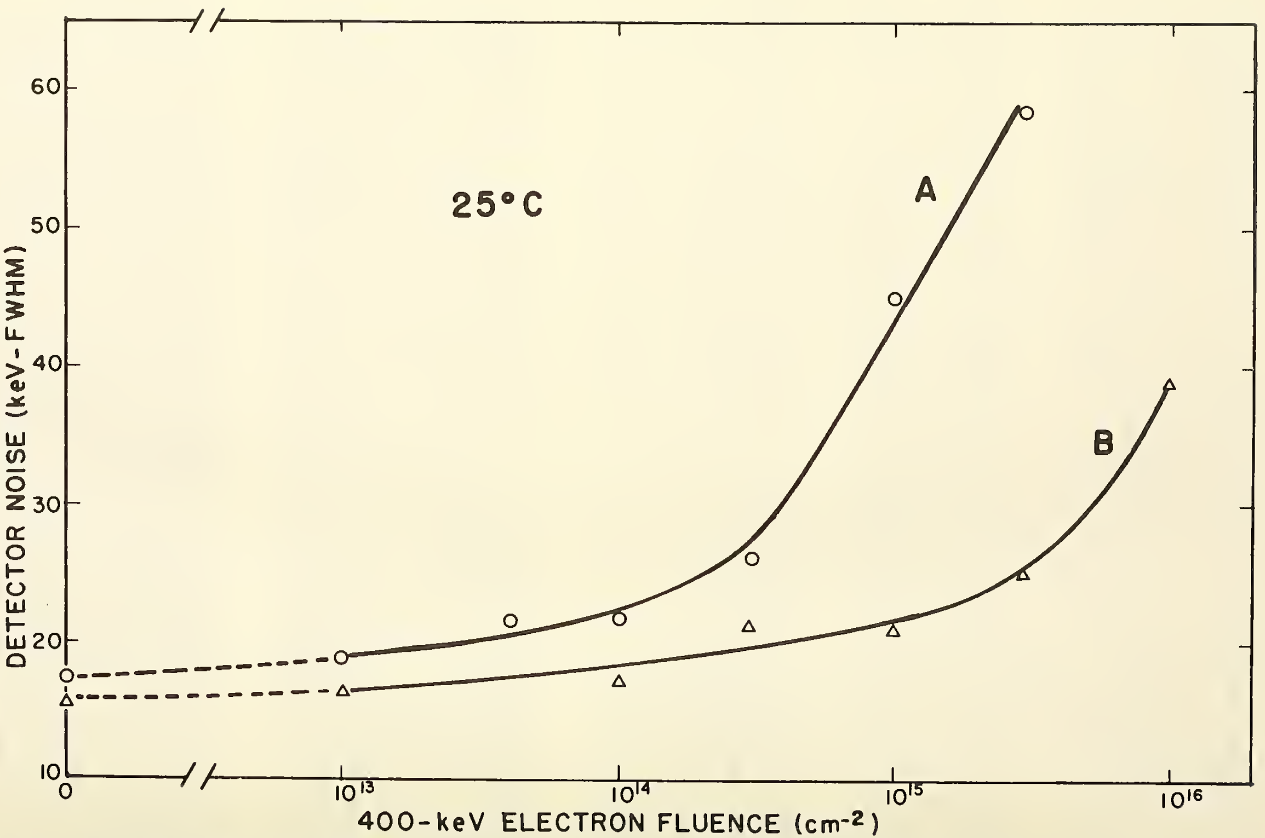

Fig. 19 Detector noise (resulting from radiation damage) as a function of the fluence of 400-keV electrons incident on the (A) gold contact and (B) aluminum contact of a 1000-μm thick, silicon, surface-barrier detector.

spectra were observed after electron fluences of 1×10^{15} cm^{-2} and 1×10^{16} cm^{-2} for irradiation of the gold and aluminum contacts, respectively. The pulse height of the secondary peak was much lower than that of the primary peak which represented nearly 100 percent charge collection efficiency. The rise time of the output signal which produced the secondary peak was very long, which suggests that charge carriers were being delayed by temporary trapping effects caused by the radiation damage. In general, the rate of detector noise degradation with fluence was lower for irradiation of the aluminum contact than for the gold contact as shown in Fig. 19. (Y. M. Liu and J. A. Coleman)

Plans: The life-test system for evaluating detectors for the Pioneer F experiments will be completed. Evaluation of detectors for the IMP satellite experiments will continue. Additional specimens of large-diameter, dislocation-free silicon will be obtained for characterization. The results of the study of electron damage effects in detectors will be analyzed in preparation for publication.

4.5 REFERENCE

4.3 Microwave Device Measurements

1. H. C. Torrey and C. A. Whitmer, *Crystal Rectifiers*, Vol. 15, MIT Radiation Laboratory Series, McGraw-Hill Co., New York, 1948.

Appendix A

JOINT PROGRAM STAFF

Coordinator: J. C. French
Consultant: C. P. Marsden

Semiconductor Characterization Section
(301) 921-3625

Dr. W. M. Bullis, Chief

A. J. Baroody, Jr.
D. L. Blackburn
F. H. Brewer
Mrs. E. C. Cohen*
M. Cosman
Dr. J. R. Ehrstein
G. G. Harman
Mrs. R. E. Joel+
H. K. Kessler
Mrs. K. O. Leedy
R. L. Mattis
Dr. W. E. Phillips
Miss T. A. Poole+
Miss D. R. Ricks
H. A. Schafft
A. W. Stallings
G. N. Stenbakken
W. R. Thurber

Semiconductor Processing Section
(301) 921-3541

Dr. J. A. Coleman, Chief

B. H. Audet
H. A. Briscoe
W. K. Croll
Mrs. S. A. Davis+
H. E. Dyson*
W. J. Keery
E. I. Klein
J. Krawczyk
T. F. Leedy
Y. M. Liu
Miss J. M. Morrison
J. Oroshnik
D. M. Skopik
Dr. A. H. Sher
L. M. Smith
G. P. Spurlock

Electron Devices Section
(301) 921-3622

J. C. French, Chief

Mrs. C. F. Bolton+
Mrs. R. Y. Cowan
Miss B. S. Hope+
R. L. Gladhill
J. M. Kenney
F. F. Oettinger
M. K. Phillips
R. C. Powell*
G. J. Rogers
S. Rubin
M. Sigman
L. R. Williams

---

* Part Time
\+ Secretary

Appendix B

COMMITTEE ACTIVITIES

ASTM Committee F-1; Materials for Electron Devices and Microelectronics
- A. J. Baroody, Lifetime Section
- F. H. Brewer, Resistivity Section
- W. M. Bullis, Editor, Subcommittee 4, Semiconductor Crystals; Leaks, Resistivity, Mobility, Dielectrics, and Compound Semiconductors Sections
- J. R. Ehrstein, Resistivity, Epitaxial Resistivity, and Epitaxial Thickness Sections
- J. C. French, Committee Editor
- T. F. Leedy, Photoresist Section
- J. Oroshnik, Thick Films and Photomasking Sections; Chairman, Thin Films Sections
- W. E. Phillips, Crystal Perfection, Encapsulation, Thin Films, and Thick Films Sections; Chairman, Lifetime Section
- A. H. Sher, Germanium Section
- M. Sigman, Editor, Subcommittee 5, Semiconductor Processing Materials
- W. R. Thurber, Mobility, Germanium, and Impurities in Semiconductors Sections

Electronic Industries Association:
- F. F. Oettinger, Associate Member, MED 32, Active Digital Circuits; Task Group 41.6, Thermal Considerations, MED 41, Physical Characterization Requirements

Joint Electron Device Engineering Council (EIA-NEMA):
- J. M. Kenney, Microwave Diode Measurements, JS-3, UHF and Microwave Diodes
- F. F. Oettinger, Thermal Resistance Measurements, JS-1, Rectifier Diodes; Technical Advisor, JS-14, Thyristors
- R. C. Powell, Microwave Diode Measurement, JS-3, UHF and Microwave Diodes; Task Group on Transistor Scattering Parameter Measurement Standards, JS-9, Low Power Transistors
- S. Rubin, Chairman, Council Task Group on Galvanomagnetic Devices
- H. A. Schafft, Consultant on Second Breakdown Specifications, JS-6, Power Transistors

IEEE Electron Devices Group:
- J. C. French, Standards Committee
- J. M. Kenney, Chairman, Standards Committee Task Group on Microwave Solid State Devices II (Mixer and Video Detector Diodes)

IEEE Nuclear Science Group:
- J. A. Coleman, Administrative Committee; Nuclear Instruments and Detectors Committee; Editorial Board, *Transactions on Nuclear Science;* Chairman, 1970 Nuclear Science Symposium

IEEE Magnetics Group:
S. Rubin, Chairman, Galvanomagnetic Standards Subcommittee

IEC TC47, Semiconductor Devices and Integrated Circuits:
F. F. Oettinger, U. S. Experts Advisory Committee
S. Rubin, Technical Expert, Galvanomagnetic Devices; U. S. Specialist for Working Group 5 on Hall Devices and Magnetoresistive Devices

NAS-NRC Ad Hoc Panel on Radiation Detectors and Associated Circuitry:
J. A. Coleman

Appendix C

SOLID-STATE TECHNOLOGY & FABRICATION SERVICES

Technical services in areas of competence are provided to other NBS activities and other government agencies as they are requested. Usually these are short-term, specialized services that cannot be obtained through normal commercial channels. Such services provided during the last quarter are listed below and indicate the kinds of technology available to the program.

1. Radiation detectors — (A. H. Sher)
   Assistance with reprocessing, mounting, and testing germanium gamma-ray detectors was provided for the Nuclear Spectroscopy and Radioactivity Sections of the Center for Radiation Research.

2. Sectioning and plating — (H. A. Briscoe)
   Transistors were sectioned, polished, and stained to reveal cross-sectional geometries and small piece parts were gold plated for the Electronic Technology Division.

3. Quartz and glass fabrication — (E. I. Klein)
   a. Ion gauges and an attenuator vacuum system were repaired and flanges were attached to vacuum tubes for the Vacuum Measurements Section.
   b. A quartz flange support for a laser tube was prepared for the Solid State Physics Section.
   c. Special metal parts were supplied for the Crystallography Section.
   d. Glass-to-metal seals were prepared for a variety of groups.

Appendix D

JOINT PROGRAM PUBLICATIONS

Prior Reports:

A review of the early work leading to this Program is given in W. M. Bullis, "Measurement Methods for the Semiconductor Device Industry—A Review of NBS Activity," NBS Tech. Note 511, December, 1969.

Quarterly reports covering the period since July 1, 1968, have been issued under the title "Methods of Measurement for Semiconductor Materials, Process Control, and Devices."

Quarter Ending	NBS Tech. Note	Date Issued	DDC Accession No.
September 30, 1968	472	December, 1968	AD 681440
December 31, 1968	475	February, 1969	AD 683803
March 31, 1969	488	July, 1969	AD 692232
June 30, 1969	495	September, 1969	AD 695820
September 30, 1969	520	March, 1970	AD 702833
December 31, 1969	527	May, 1970	

Current Publications:

A. H. Sher and W. J. Keery, "Variation of the Effective Fano Factor in a Ge(Li) Detector," *IEEE Trans. Nucl. Sci.* NS-17, 1, 39-43 (February, 1970).

A. H. Sher and J. A. Coleman, "Lithium Driftability in Detector Grade Germanium," *IEEE Trans. Nucl. Sci.* NS-17, 3, 125-129 (June, 1970).

J. A. Coleman, "Material Limitations on the Performance of Semiconductor Nuclear Radiation Detectors," presented at 12th Scintillation and Semiconductor Counter Symposium, Washington, March, 1970; to appear in *IEEE Trans. Nucl. Sci.*, August, 1970.

R. C. Powell, "Precision Coaxial Connectors," a chapter to be published in *Advances in Microwaves* (Academic Press).

J. Oroshnik and W. K. Croll, "Thin Film Adhesion Testing by the Scratch Method," accepted for presentation at the Surface Science Symposium, Americal Vacuum Society, New Mexico Section, April 22, 1970.

W. R. Thurber, "Determination of Oxygen Concentration in Silicon and Germanium by Infrared Absorption," NBS Tech. Note 529, May, 1970.

Latest developments in the subject area of this publication, as well as in other areas where the National Bureau of Standards is active, are reported in the NBS Technical News Bulletin. See following page.

HOW TO KEEP ABREAST OF NBS ACTIVITIES

Your purchase of this publication indicates an interest in the research, development, technology, or service activities of the National Bureau of Standards.

The best source of current awareness in your specific area, as well as in other NBS programs of possible interest, is the TECHNICAL NEWS BULLETIN, a monthly magazine designed for engineers, chemists, physicists, research and product development managers, librarians, and company executives.

If you do not now receive the TECHNICAL NEWS BULLETIN and would like to subscribe, and/or to review some recent issues, please fill out and return the form below.

Mail to: Office of Technical Information and Publications
National Bureau of Standards
Washington, D. C. 20234

Name ______________________________

Affiliation ______________________________

Address ______________________________

City ____________________ State __________ Zip __________

☐ Please send complimentary past issues of the Technical News Bulletin.

☐ Please enter my 1–yr subscription. Enclosed is my check or money order for $3.00 (additional $1.00 for foreign mailing).
Check is made payable to: SUPERINTENDENT OF DOCUMENTS.

☆ U. S. GOVERNMENT PRINTING OFFICE : 1970—431-991/86

NBS TECHNICAL PUBLICATIONS

PERIODICALS

JOURNAL OF RESEARCH reports National Bureau of Standards research and development in physics, mathematics, chemistry, and engineering. Comprehensive scientific papers give complete details of the work, including laboratory data, experimental procedures, and theoretical and mathematical analyses. Illustrated with photographs, drawings, and charts.

Published in three sections, available separately:

• Physics and Chemistry

Papers of interest primarily to scientists working in these fields. This section covers a broad range of physical and chemical research, with major emphasis on standards of physical measurement, fundamental constants, and properties of matter. Issued six times a year. Annual subscription: Domestic, $9.50; foreign, $11.75*.

• Mathematical Sciences

Studies and compilations designed mainly for the mathematician and theoretical physicist. Topics in mathematical statistics, theory of experiment design, numerical analysis, theoretical physics and chemistry, logical design and programming of computers and computer systems. Short numerical tables. Issued quarterly. Annual subscription: Domestic, $5.00; foreign, $6.25*.

• Engineering and Instrumentation

Reporting results of interest chiefly to the engineer and the applied scientist. This section includes many of the new developments in instrumentation resulting from the Bureau's work in physical measurement, data processing, and development of test methods. It will also cover some of the work in acoustics, applied mechanics, building research, and cryogenic engineering. Issued quarterly. Annual subscription: Domestic, $5.00; foreign, $6.25*.

TECHNICAL NEWS BULLETIN

The best single source of information concerning the Bureau's research, developmental, cooperative and publication activities, this monthly publication is designed for the industry-oriented individual whose daily work involves intimate contact with science and technology—*for engineers, chemists, physicists, research managers, product-development managers, and company executives*. Annual subscription: Domestic, $3.00; foreign, $4.00*.

* Difference in price is due to extra cost of foreign mailing.

NONPERIODICALS

Applied Mathematics Series. Mathematical tables, manuals, and studies.

Building Science Series. Research results, test methods, and performance criteria of building materials, components, systems, and structures.

Handbooks. Recommended codes of engineering and industrial practice (including safety codes) developed in cooperation with interested industries, professional organizations, and regulatory bodies.

Special Publications. Proceedings of NBS conferences, bibliographies, annual reports, wall charts, pamphlets, etc.

Monographs. Major contributions to the technical literature on various subjects related to the Bureau's scientific and technical activities.

National Standard Reference Data Series. NSRDS provides quantitative data on the physical and chemical properties of materials, compiled from the world's literature and critically evaluated.

Product Standards. Provide requirements for sizes, types, quality and methods for testing various industrial products. These standards are developed cooperatively with interested Government and industry groups and provide the basis for common understanding of product characteristics for both buyers and sellers. Their use is voluntary.

Technical Notes. This series consists of communications and reports (covering both other agency and NBS-sponsored work) of limited or transitory interest.

Federal Information Processing Standards Publications. This series is the official publication within the Federal Government for information on standards adopted and promulgated under the Public Law 89–306, and Bureau of the Budget Circular A–86 entitled, Standardization of Data Elements and Codes in Data Systems.

Order NBS publications from: Superintendent of Documents
Government Printing Office
Washington, D.C. 20402

U.S. DEPARTMENT OF COMMERCE
WASHINGTON, D.C. 20230

OFFICIAL BUSINESS

Penalty for Private Use, $300

POSTAGE AND FEES PAID
U.S. DEPARTMENT OF COMMERCE